

Identification of Imidazo-Pyrrolopyridines as Novel and Potent JAK1 Inhibitors

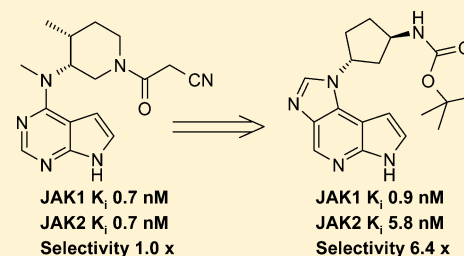
Janusz J. Kulagowski,^{*,†} Wade Blair,^{§,▽} Richard J. Bull,[†] Christine Chang,[§] Gauri Deshmukh,[⊥] Hazel J. Dyke,[†] Charles Eigenbrot,[○] Nico Ghilardi,[#] Paul Gibbons,^{||} Trevor K. Harrison,[†] Peter R. Hewitt,[†] Marya Liimatta,[§] Christopher A. Hurley,[†] Adam Johnson,[§] Tony Johnson,[†] Jane R. Kenny,[⊥] Pawan Bir Kohli,[§] Robert J. Maxey,[†] Rohan Mendonca,^{||} Kyle Mortara,[○] Jeremy Murray,[○] Raman Narukulla,[†] Steven Shia,[○] Micah Steffek,[○] Savita Ubhayakar,[⊥] Mark Ultsch,[○] Anne van Abbema,[§] Stuart I. Ward,[†] Bohdan Waszkowycz,^{‡,◆} and Mark Zak^{||}

[†]Departments of Medicinal Chemistry and [‡]Computer Aided Drug Design, Argenta, 8/9 Spire Green Centre, Harlow CM19 5TR, United Kingdom

[§]Departments of Biochemical and Cellular Pharmacology, ^{||}Discovery Chemistry, [⊥]Drug Metabolism and Pharmacokinetics, [#]Immunology, and [○]Structural Biology, Genentech, Inc., 1 DNA Way, South San Francisco, California 94080, United States

Supporting Information

ABSTRACT: A therapeutic rationale is proposed for the treatment of inflammatory diseases, such as rheumatoid arthritis (RA), by specific targeting of the JAK1 pathway. Examination of the preferred binding conformation of clinically effective, pan-JAK inhibitor **1** led to identification of a novel, tricyclic hinge binding scaffold **3**. Exploration of SAR through a series of cycloamino and cycloalkylamino analogues demonstrated this template to be highly tolerant of substitution, with a predisposition to moderate selectivity for the JAK1 isoform over JAK2. This study culminated in the identification of subnanomolar JAK1 inhibitors such as **22** and **49**, having excellent cell potency, good rat pharmacokinetic characteristics, and excellent kinase selectivity. Determination of the binding modes of the series in JAK1 and JAK2 by X-ray crystallography supported the design of analogues to enhance affinity and selectivity.



INTRODUCTION

The Janus protein tyrosine kinases (JAK1, JAK2, JAK3, and TYK2) mediate intracellular signaling of numerous cytokines and thereby play critical roles in a variety of biological processes, including hematopoiesis and the regulation of immune and inflammatory responses.¹ JAKs constitutively associate with cytoplasmic motifs in the intracellular domain of cytokine receptors and are activated upon ligand induced receptor homo- or heterodimerization, which results in the immediate phosphorylation of tyrosine residues within the cytoplasmic domain of the receptors. These phosphotyrosines then serve as docking sites for cytoplasmic signal transducer and activator of transcription (STAT) proteins. Upon recruitment to the receptor complex, STATs become phosphorylated by the JAKs, which allow them to dimerize and travel to the cellular nucleus, where they act as transcription factors.²

Biochemical and genetic studies have shown that JAK1 is the most broadly used JAK, as it is involved in the signaling of the gamma common (γ_c), beta common (β_c), gp130, type I and type II interferon, IL-6, and IL-10 subfamilies of cytokines.^{1a,3} JAK2 utilization is more restricted and generally associated with receptors that function as homodimers, such as the erythropoietin (EPO) and growth hormone receptors, among others. Consistent with its role in EPO signaling, mice lacking

the JAK2 gene die of anemia,^{2a} while a gain-of-function mutation in the JAK2 gene ($JAK2^{V617F}$) results in polycythemia vera and other myeloproliferative disorders (MPD) in humans.⁴ Similar to JAK1 and JAK2, TYK2 is also widely expressed and activated by numerous cytokines. In contrast to JAK1 and JAK2, however, deficiency in TYK2 is not lethal, suggesting that TYK2 might be more dispensable than JAK1 and JAK2. While TYK2-deficient mice show no gross abnormalities in the absence of challenge, TYK2-deficient humans suffer from hyper IgE syndrome but are otherwise viable.⁵ Finally, JAK3 is the only JAK family member with a restricted expression pattern and function, being localized in lymphoid tissue.⁶ This protein associates exclusively with the γ_c chain, and in both humans and mice, JAK3 deficiency phenocopies γ_c deficiency, resulting in X-linked severe combined immunodeficiency (X-SCID) due to complete abrogation of IL-2, IL-4, IL-7, IL-9, IL-15, and IL-21 signaling.⁷

Owing to its restriction to the γ_c subfamily of cytokines, JAK3 has long been viewed as an attractive therapeutic target for the treatment of certain immune system indications (e.g., transplant rejection and rheumatoid arthritis (RA)).^{7,8} Initially

Received: March 29, 2012

Published: May 16, 2012

described as a JAK3 specific inhibitor,^{8b} the small molecule tofacitinib (**1**, CP-690,550; Figure 1) is now in advanced clinical

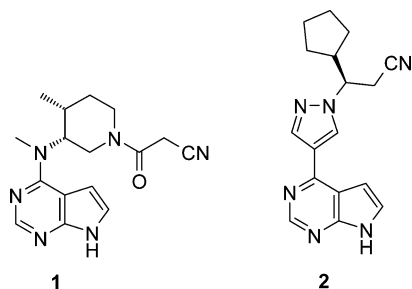


Figure 1. JAK inhibitors in advanced clinical evaluation.

testing and has demonstrated efficacy against RA, psoriasis, Crohn's disease, kidney transplant rejection, and ulcerative colitis.⁹ It has recently become clear that **1** is not as specific as initially thought for JAK3, but rather is a potent pan-JAK inhibitor ($K_i = 0.68, 0.99, 0.24,$ and 4.39 nM for JAK1, JAK2, JAK3, and TYK2, respectively).¹⁰ Multiple inhibitors targeting JAK2 are also undergoing clinical evaluation against MPDs, and several have exhibited promising results.^{4,11} Of these agents, ruxolitinib (**2**, INCB018424; Figure 1) was approved in 2011 for the treatment of myelofibrosis,¹² and the compound has also demonstrated efficacy in the RA setting.¹³ The reported potency of ruxolitinib (**2**) for JAK3 is far weaker than its inhibitory activity toward the other JAK family members ($IC_{50} = 3.3, 2.8, 428,$ and 19 nM for JAK1, JAK2, JAK3, and TYK2, respectively),¹⁴ suggesting that the compound's clinical efficacy against RA is unlikely to be driven by inhibition of the JAK3 isoform. Furthermore, a recent report claims that for cytokine signaling mediated through γ_c -containing receptors, the JAK1 pathway is dominant over JAK3.¹⁵

Both **1** and **2** are potent inhibitors of JAK1 and JAK2, but differ in their potency for JAK3 and TYK2. Since both have exhibited activity against RA, we hypothesized that this property was a result of JAK1 inhibition as a result of the following considerations. First, while IL-6 stimulation activates JAK1, JAK2, and TYK2, cells taken from JAK1 knockout mice exhibit substantially reduced levels of responsiveness when compared to those from wild-type animals.¹⁶ In contrast, comparable activities toward IL-6 are observed between wild-type and knockout mice in the case of both JAK2¹⁷ and TYK2.¹⁸ Second, tocilizumab, an IL-6R-specific, neutralizing humanized monoclonal antibody, has shown impressive clinical efficacy in the treatment of RA.¹⁹ Furthermore, JAK1 rather than JAK2 participates in the signaling of pathophysiologically relevant γ_c cytokines, including IL-15, neutralization of which also results in improvement of RA.²⁰

Anemia has been observed in some patients during clinical evaluation of both **1**²¹ and **2**.²² As noted above, both compounds exhibit potent JAK2 inhibitory activity, and a link between JAK2 deficiency and anemia has been demonstrated in mice.^{22a,23} Therefore, we reasoned that a JAK1 selective, JAK2 sparing inhibitor would constitute an ideal therapeutic agent to target inflammatory disorders such as RA.²⁴ Herein we describe the identification and characterization of a novel series of tricyclic JAK inhibitors along with our initial efforts at achieving the desired JAK1/JAK2 selectivity profile within this chemotype.

RESULTS AND DISCUSSION

Molecular modeling studies previously performed on compound **1** indicated that a staggered, *anti*-periplanar conformation (*anti*-**1**, Figure 2), in which the *N*-methyl group points toward the pyrrole ring, is energetically favored over the alternate rotational isomer (*syn*-**1**, Figure 2).²⁵ Furthermore, a single crystal X-ray structure determination of a closely related derivative indicated this compound also exists in a similar staggered conformation.²⁶ In contrast, an X-ray cocrystal structure of **1** bound to JAK1 clearly showed the piperidine moiety residing in an eclipsed, *syn*-periplanar orientation to the bicyclic ring system (*syn*-**1**, Figure 2).²⁷ These observations suggested the use of a tricyclic template to rigidify the inhibitor structure in a manner that would closely mimic the compound **1** rotamer that was preferred for JAK1 binding. We elected to explore this possibility by introducing an imidazole ring into the bicyclic inhibitor design, giving rise to an imidazo-pyrrolopyridine scaffold (e.g., **3**, Figure 1).²⁸

At the outset of this work, it was reasoned that, in order to be considered potential drug candidates, any new compounds should possess levels of biochemical and functional JAK1 potency comparable to **1**. Specifically, the goal was to achieve at least low single-digit and, preferably, subnanomolar biochemical activity, with a cellular EC_{50} value ideally less than 100 nM. However, the degree of selectivity for JAK1 over JAK2 that would be required to impart therapeutic benefit relative to **1** was unclear. The observation of reduced hemoglobin levels at higher (>5 mg BID) doses of **1** during a recent clinical trial was attributed by the authors to possible effects on hematopoiesis through inhibition of JAK2.^{21b} This led us to surmise that a relatively modest degree of selectivity for JAK1 over JAK2, perhaps on the order of 10-fold, may be sufficient to provide a suitable therapeutic window.

To the best of our knowledge, no account of how JAK1 selectivity may be achieved has thus far been disclosed, although compounds with this profile have been described in recent patent applications.²⁹ Moreover, a compound (GLPG0634; structure undisclosed), reported to be JAK1 selective ($IC_{50} = 10, 28, 81,$ and 116 nM for JAK1, JAK2, JAK3, and TYK2, respectively),³⁰

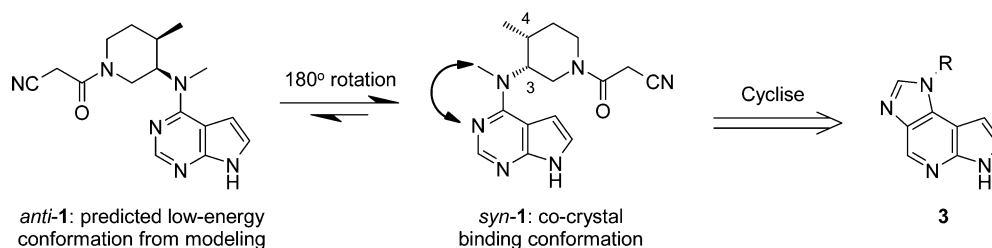
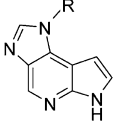
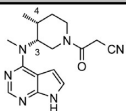
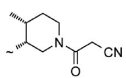
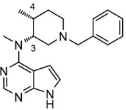
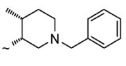
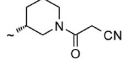
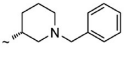
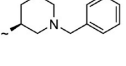
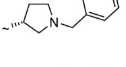
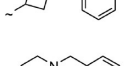
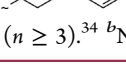


Figure 2. Generation of tricyclic inhibitor scaffold **3**.

Table 1. JAK Isoform Inhibitory Activities of Heterocycloamine Derivatives of 3



Ex	Stereo-chemistry	R	^a JAK1 K _i (nM)	^a JAK2 K _i (nM)	^a JAK3 K _i (nM)	^a TYK2 K _i (nM)
1	3 <i>R</i> , 4 <i>R</i>		0.7	0.7	0.4	7.8
4	(+/-)		0.5	0.3	0.9	4.2
5	3 <i>R</i> , 4 <i>R</i>		610	770	120	3500
6	(+/-)		12	25	22	160
7	<i>R</i>		0.4	1.2	3.8	4.7
8	<i>R</i>		24	56	130	250
9	<i>S</i>		88	47	220	71
10	<i>R</i>		15	25	130	89
11	^b NA		62	59	200	540
12	NA		2.4	4.4	33	85

^aArithmetic mean of at least 3 separate determinations ($n \geq 3$).³⁴ ^bNot applicable.

has recently demonstrated efficacy against RA with a good safety profile in an early phase II trial.³¹ Furthermore, diamino-1,2,4-triazoles structurally related to JNJ-7706621 (IC₅₀ = 39, 1700, 950, and 39 nM for JAK1, JAK2, JAK3, and TYK2, respectively) have been reported to also be selective for JAK1 and TYK2 over the other JAK isoforms,³² although the reference compound is known to be somewhat promiscuous against a variety of other kinases.³³

In our biochemical assays,³⁴ compound **1** was confirmed to be a potent, pan-JAK inhibitor with some selectivity over TYK2 (Table 1). Gratifyingly, the racemic tricyclic molecule **4** displayed similar inhibitory properties when tested against the same enzymes. Equally striking was the observation that, while **5** (Figure 3), an *N*-benzyl-containing compound related to **1**, was several hundred-fold less potent, the corresponding tricyclic inhibitor **6** suffered only an order of magnitude loss in activity. These observations suggested that the tricyclic imidazopyrrolopyridine scaffold could possess a divergent and productive SAR when compared to pyrrolopyrimidine-containing inhibitors such as **1**. Simplification of **4** by the removal of the piperidinyl methyl group afforded **7**, which maintained excellent JAK1 potency.

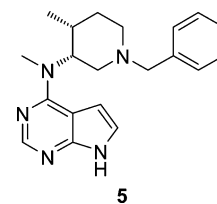


Figure 3. Synthetic precursor to **1**.

Encouraged by these preliminary results, we sought alternatives to the distinctive cyanoacetamide substituent present in **1**, **4**, and **7**. Capitalizing on the favorable results observed for **6**, we examined different ring systems that retained the *N*-benzyl group (Table 1). The subtle contribution to JAK binding of the piperidinyl methyl group present in **6** was demonstrated by the *des*-methyl analogue **8** (2–6-fold loss in potency across the four isoforms), while **9** confirmed that the (*R*)-piperidine configuration favored JAK1 activity. Replacement of the piperidine in **8** with the corresponding *N*-benzyl pyrrolidine and azetidine had minimal impact on inhibitory potency across the four JAK family enzymes in our testing

panel (10 and 11, respectively). However, incorporation of an achiral 4-substituted piperidine into the tricyclic inhibitor design (12) resulted in a dramatic increase in JAK potency relative to the 3-substituted piperidines 8 and 9.

Having identified compounds such as 7 and 12 with encouraging JAK inhibitory potency, further optimization of this novel series of tricyclic JAK inhibitors was undertaken. Following the determination of enzyme activity against all four isoforms, compounds were assessed for cellular potency and selectivity. Since the general pattern of isoform activity displayed in Table 1, namely higher inhibition at JAK1 and JAK2 than at JAK3 and TYK2, was maintained in subsequent examples, further discussion of biochemical potency against the latter two enzymes will be omitted for the purpose of brevity. JAK1 enzyme (biochemical) selectivity is expressed as the ratio: JAK2 (K_i)/JAK1 (K_i). With regard to cellular potency, it was considered desirable to determine both JAK1 and JAK2 cellular activity in the same cell line, in order to circumvent any issues arising from differences in response between alternate cell types. In TF-1 cells, IL-6 stimulation leads to STAT3 phosphorylation predominantly through involvement of JAK1, whereas EPO stimulation elaborates phospho-STAT5 in a JAK2 dependent fashion.³⁴ By analogy to enzyme selectivity, quoted cell selectivities are the ratios of pSTAT5 EC₅₀ over pSTAT3 EC₅₀. Compounds were also routinely evaluated for metabolic stability by incubation with human liver microsomes. Reference standard 1 exhibited excellent cell potency in the IL-6-driven pSTAT3 cell assay (Table 2). Despite having comparable JAK1 biochemical potency, tricyclic analogue 7 exhibited somewhat weaker cell potency, but equivalent microsomal stability to 1. Although having somewhat reduced activity for JAK1 relative to 7, 12 proved more potent in the JAK1-pSTAT3 cellular assay. However, *in vitro* turnover in human microsomes was observed to be higher for 12 than that noted for 7. Despite this shortcoming, the 4-piperidinyl regioisomer was selected for further optimization, on the basis that a cyanoacetyl substituent was not required, as demonstrated by the excellent JAK1 enzyme potency of 12, and the fact that this positional isomer was less stereochemically complex by virtue of not possessing a chiral center. Reasoning that the high *in vitro* clearance observed with 12 was due to the presence of a lipophilic benzyl group, efforts were undertaken to address this liability. Unsubstituted piperidine 13 suffered a significant loss in JAK1 inhibitory activity, with a concomitant loss in cellular potency. Introduction of polarity into 12 in the form of a pyrimidine (14) maintained comparable inhibitory activity, while concurrently reducing degradation in human microsomal preparations. These improvements unfortunately came at the expense of cellular potency when compared to the less polar 12. The cyanoacyl substituent present in 1, 4, and 7 was significantly less successful when introduced in the context of the 4-piperidine (15), especially in terms of cellular activity. A benzoyl 4-piperidine substituent likewise proved to be a poor replacement for benzyl (16). No JAK1 potency advantage was offered by a simple alkyl amide (17), although JAK1 enzyme potency was maintained relative to 12 and 14 with sulfonamide 19 and, to a lesser extent, 18. Interestingly, substitution of the 4-piperidine with a simple alkyl group, as in 20, was highly detrimental to activity. However, functionalization of the alkyl group with electron-withdrawing moieties proved to be a particularly successful strategy, with both JAK1 enzyme and cell potency being restored in the trifluoroethyl analogue 21. Within this series of compounds, cyanoethyl derivative 22 encompassed the optimum overall balance

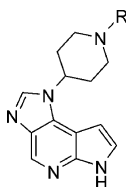
of properties, with excellent cell potency and high *in vitro* metabolic stability.

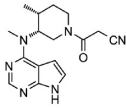
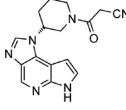
Some general observations on the tricyclic compounds discussed thus far warrant comment. 4-Piperidine tolerated a wide range of substituents; the varied chemotypes contained in Table 2 span only a 100-fold range in JAK1 inhibitory activity. The tricyclic scaffold also appeared to have an intrinsic preference for JAK1; nearly all of the compounds displayed a very modest but consistent selectivity for this isoform over JAK2 in the biochemical assays. Furthermore, excellent JAK1-pSTAT3 cell potency was achievable with the tricyclic inhibitors. Cell and biochemical selectivities were in good agreement for the most part, with perhaps a subtle enhancement of the former relative to the latter, as observed also with 1. Derivatization of the piperidine with dimethyl glycine (23) resulted in some loss in enzyme activity, but an improvement in biochemical selectivity, when compared to the isosteric amide (17). This characteristic was observed with other derivatives bearing a basic center in this vicinity, with cyclization (24–27) generally offering some benefit to both biochemical potency and selectivity. For instance, proline derivative 26 displayed a 17-fold preference for JAK1 over JAK2. Possible reasons for the enhanced selectivity observed with compounds incorporating a basic, pendent substituent are discussed in more detail below. Unfortunately, despite possessing intriguing levels of selectivity, progression of this subset of compounds was precluded by a persistent inability to achieve required levels of inhibitory activity, leading to commensurately poor cellular potency.

With the aim of enhancing binding interactions by exploiting potential lipophilic contacts between the piperidine ring and protein residues located under the P-loop (see discussion of crystallographic studies below), each position on the ring was sequentially probed with a methyl group. Incorporation of a methyl group in both *cis* and *trans* dispositions at either the 2- or 3-positions on the piperidine ring provided no significant benefit (data not shown); however, a distinct trend emerged when this substituent was located at the 4-position (Table 3). Although this change generally reduced JAK1 enzyme potency relative to the corresponding unmethylated counterparts, the extent was dramatically dependent on *N*-substitution. Thus, sulfonamide 30 was equipotent to its unmethylated analogue 19, whereas 32 suffered a 50-fold reduction in activity when compared to 22. However, in each case, biochemical selectivity over JAK2 was improved relative to the unsubstituted example, although this effect was variable, ranging from 3-fold for 32 to 16-fold for 28. The general reduction in activity observed on methylation of the piperidine also translated to the cellular assay; of the compounds tested, only 30 displayed moderate potency.

In an effort to improve further upon the properties of the compounds described thus far, a series of substituted cyclohexylamines was also explored. For structural simplicity, and by analogy with the findings from an evaluation of piperidine SAR, attention in this case was focused on the 1,4-disubstituted regioisomer. Additionally, a selection of *cis* and *trans* stereoisomeric pairs was examined in order to establish stereochemical preference.

Although identical JAK1 inhibitory activity was exhibited by *tert*-butyl carbamates 33 and 34 (Table 4), a marginal preference for the *trans* over *cis* isomer was observed in the case of the unsubstituted amine (35 and 36, respectively). However, this trend was far more pronounced in the morpholine substituted pair, with the *trans* isomer 37 significantly more potent

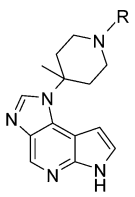
Table 2. *In Vitro* Properties of 4-Piperidinyl Derivatives of 3


Ex	R	^a JAK1 K _i (nM)	^b JAK1 Enzyme Selectivity	^{a,c} JAK1 Cell EC ₅₀ (nM)	^d JAK1 Cell Selectivity	^e Hum Mic T _{1/2} (h)
1		0.7	1.0	53	1.8	1.7
7		0.4	2.2	180	4.8	1.4
12		2.4	1.9	86	3.1	0.8
13	H	45	5.6	1400	^f >6.3	^g ND
14		2.0	2.3	350	2.8	4.0
15		19	2.3	>10000	ND	2.0
16		18	2.2	1300	3.1	1.4
17		28	2.6	1800	3.2	0.5
18		9.6	1.0	540	2.2	0.7
19		1.2	2.5	140	5.9	2.2
20		50	3.2	520	5.1	2.5
21		2.9	2.0	160	3.5	3.8
22		0.6	1.8	43	4.6	7.5
23		32	7.7	>7100	ND	1.5
24		43	9.1	ND	ND	2.8
25		15	9.0	>8600	ND	4.7
26		22	17	>8800	ND	1.3
^h 27		11	10	1800	>5.5	3.5

^aArithmetic mean of at least 3 separate determinations ($n \geq 3$). ^bBiochemical selectivity for JAK1 over JAK2 (JAK2 K_i/JAK1 K_i). ^cpSTAT3-IL6 JAK1 driven TF-1 cell-based assay. ^dCell-based selectivity for JAK1 over JAK2 (pSTAT5-EPO EC₅₀/pSTAT3-IL6 EC₅₀). ^eHalf-life in the presence of *in vitro* preparations of human liver microsomes. ^fFrom ref 35. ^gNot determined. ^hSingle, more active enantiomer; absolute configuration was assigned arbitrarily.

than the *cis* isomer 38. The *trans* diastereomer also possessed superior cell potency in the case of the *t*-butyl carbamate (33, 34) and morpholine (37, 38) pairs, although not for

amines 35 and 36. Indeed, both latter compounds displayed very similar profiles, having moderate biochemical and cell potencies, but high (12-fold) JAK1 cellular selectivities.

Table 3. *In Vitro* Properties of 4-Methylated Piperidinyl Derivatives of 3


Ex	R	^a JAK1 K _i (nM)	^b JAK1 Enzyme Selectivity	^{a,c} JAK1 Cell EC ₅₀ (nM)	^d JAK1 Cell Selectivity	^e Hum Mic T _{1/2} (h)
28	H	96	16	880	>11	>10
29		8.3	5.2	670	9.7	1.6
30		1.7	6.5	210	10	>10
31		33	4.0	ND	ND	1.6
32		50	3.1	ND	ND	2.3

^aMean of at least 3 separate determinations ($n \geq 3$). ^bBiochemical selectivity for JAK1 over JAK2 (JAK2 K_i/JAK1 K_i). ^cpSTAT3-IL6 JAK1 driven TF-1 cell-based assay. ^dCell-based selectivity for JAK1 over JAK2 (pSTAT5-EPO EC₅₀/pSTAT3-IL6 EC₅₀). ^eHalf-life in the presence of *in vitro* preparations of human liver microsomes.

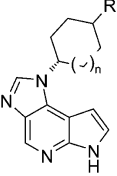
However, further evaluation of 35 indicated that this compound had poor rat pharmacokinetic characteristics (see below).

Derivatization of 35 provided a range of substituents broadly comparable to those applied to the piperidines in Table 2. Similar tolerance of a broad range of substitution was also observed with the examples listed in Table 4. Amide 39, amines 40–42, and sulphonamide 43 all possessed single or low double digit nanomolar potency for JAK1 but with variable cellular selectivities. Although having a compelling pharmacological profile, carbamate 33 displayed only moderate microsomal stability. Reasoning 33 was compromised by its high lipophilicity (logD_{7.2} 3.2), we sought to address this issue by preparing the corresponding methyl analogue 44 (logD_{7.2} 1.9). While this change dramatically improved metabolic stability, it proved detrimental to both enzyme and cell potency and selectivity, relative to 33. Interestingly, *N*-methylation of the carbamate (45) had minimal impact on potency but appeared to abolish both biochemical and cell selectivity. Seeking to reduce hydrophobicity further, the cycloalkyl moiety was truncated to a cyclopentyl ring. Racemic *trans* derivative 46 (logD_{7.2} 1.2) displayed a 3-fold improvement in JAK1 biochemical activity over 44, with a similar enhancement in cell potency. Further improvement in cell potency and selectivity was realized on reinstatement of a *t*-butyl carbamate (47) but with no penalty in metabolic stability relative to 46. The corresponding *cis* analogue 48 was less successful, both in terms of potency and stability. Resolution of 47 provided 49 as the more active enantiomer. With subnanomolar enzyme activity against JAK1, this compound also proved to have excellent potency in the pSTAT3 cell assay, with an overall profile comparable to that of 1. However, in contrast to the potent but unselective 1, compound 49 displayed moderate selectivity for the JAK1 isoform over JAK2, both in biochemical and cell-based assays, in addition to a superior microsomal stability profile.

Selected compounds were subjected to more stringent evaluation, including pharmacokinetic profiling in rat and determination of off-target selectivity (Table 5). *In vivo* plasma clearance following IV dose was high for all compounds. This was unlikely to be as a result of extensive tissue distribution

since the volume of distribution for most examples was moderate, save for compounds 12 and 35, for which the much higher values were presumably a reflection of their overtly basic nature. Despite high clearance, reasonable plasma exposure was achieved following PO dose for some compounds, depending on the balance of properties. A similar profile was previously reported for 1.²⁶ The poor oral exposure of 7 was in keeping with low MDCK apparent permeability, which likely resulted from a combination of low lipophilicity (logD) and high polarity (TPSA). In contrast, *N*-benzyl piperidine 12 exhibited excellent permeability, but its high lipophilicity and low polarity resulted in high *in vitro* turnover, with correspondingly high *in vivo* clearance, culminating in a very poor rat PK profile. These results suggested that an appropriate balance between logD and TPSA was required in order to achieve an appropriate level of permeability with perhaps some modulation of clearance in support of a favorable PK profile. Compounds 19, 30, and 41 possessed near identical logD and TPSA values (intermediate between those of 7 and 12) and consequently displayed similar permeability. The PK characteristics of all three compounds showed a substantial improvement over those of 7 and 12, with 19 and 30 in particular having good exposure and oral bioavailability. Although having comparable and moderate TPSA, 22 and 35 exhibited widely disparate PK parameters. The higher lipophilicity of 22 conveyed an excellent overall profile, whereas that of 35 was compromised by its remarkably low logD and poor apparent permeability, despite having lower clearance. Likewise, although both 12 and 49 are very lipophilic, this potential liability is offset to some extent by the significantly higher polarity of the latter, resulting in 49 having very favorable PK properties.

To assess pan-kinase selectivity, compounds were screened at a concentration 100-fold higher than their JAK1 K_i against a commercial panel of 50 (183 in the case of 7) kinases. Compounds were scored by the number of proteins showing >50% inhibition. On this basis, 7, 22, and 49 proved to have excellent selectivity against non-JAK kinases, while 35 and 41 were less selective.

Table 4. *In Vitro* Properties of Cycloalkylamine Derivatives of 3


Ex	n	R	^a Rel. Stereo	^b JAK1 K _i (nM)	^c JAK1 Enzyme Selectivity	^{b,d} JAK1 Cell EC ₅₀ (nM)	^e JAK1 Cell Selectivity	^f Hum Mic T _{1/2} (h)
33	1		<i>trans</i>	6.1	4.1	180	11	1.5
34	1		<i>cis</i>	6.1	3.2	500	3.7	^g ND
35	1		<i>trans</i>	5.8	5.8	340	12	3.7
36	1		<i>cis</i>	9.8	11	260	12	5.5
37	1		<i>trans</i>	12	2.7	180	2.0	6.8
38	1		<i>cis</i>	280	1.7	5200	1.6	3.7
39	1		<i>trans</i>	11	2.7	410	4.9	2.7
40	1		<i>trans</i>	9.3	7.8	130	8.8	4.7
41	1		<i>trans</i>	4.5	3.4	440	6.7	5.0
42	1		<i>trans</i>	5.9	3.2	180	3.6	0.8
43	1		<i>trans</i>	2.7	1.7	700	4.6	1.8
44	1		<i>trans</i>	9.5	2.4	400	4.6	>10
45	1		<i>trans</i>	13	1.0	670	0.9	>10
^h 46	0		<i>trans</i>	3.2	3.5	150	4.9	5.8
^h 47	0		<i>trans</i>	2.2	5.6	91	10	5.5
^h 48	0		<i>cis</i>	3.7	8.8	270	7.9	1.8
ⁱ 49	0		<i>trans</i>	0.9	6.4	62	9.2	5.6

^aRelative stereochemistry of substituents on the cyclohexane or cyclopentane ring. ^bMean of at least 3 separate determinations ($n \geq 3$). ^cBiochemical selectivity for JAK1 over JAK2 (JAK2 K_i/JAK1 K_i). ^dpSTAT3-IL6 JAK1 driven TF-1 cell-based assay. ^eCell-based selectivity for JAK1 over JAK2 (pSTAT5-EPO EC₅₀/pSTAT3-IL6 EC₅₀). ^fHalf-life in the presence of *in vitro* preparations of human liver microsomes. ^gNot determined. ^hRacemic. ⁱSingle, more active enantiomer; absolute configuration was assigned arbitrarily.

■ X-RAY CRYSTALLOGRAPHIC STUDIES

X-ray crystallography proved useful in establishing the binding mode of various members of the imidazo-pyrrolopyridine series and interpreting SAR trends across the JAK isoforms. The X-ray structures of **1** bound to all four JAK isoforms have been reported in the literature.^{27,36} Consistent with its pan-JAK activity, **1** exhibits a similar binding mode to all four JAK isoforms. A high degree of sequence homology exists between JAK1 and JAK2 within the ATP-binding site (Figure 4). Amino

acids in close contact to the ligand are conserved or show modest changes (e.g., JAK1 Phe958 → JAK2 Tyr931 on the hinge region). More significant differences arise in solvent-exposed residues at the periphery of the binding site, including Arg879 → Gln853, Glu966 → Asp939, and Lys965 → Arg938. Although there are several changes to P-loop residues (e.g., Glu883 → Lys857, His885 → Asn859), the side chains point away from the ligand and hence are not likely to be amenable for the design of direct hydrogen bonding contacts. The high

Table 5. Physicochemical, *in Vitro*, and Rat Pharmacokinetic Properties of Selected Compounds

Ex	logD ^a	TPSA (Å ²)	MDCK A:B P _{app} (×10 ⁻⁶ cm/s) ^b	rat Hep. T _{1/2} (h) ^c	<i>in vivo</i> rat PK ^d					kinase select. (>50% inhib.) ^e
					CL (mL/min/kg) ^f	AUC (μM·h) ^g	C _{max} (μM) ^h	V _{ss} (L/kg) ⁱ	F (%) ^j	
1 ^k		88			62		0.7		27	
7	0.39	90	0.3	>10	85	0.3	0.05	1.87	5	2/183
12	2.90	49	32.3	0.5	170	^l BLQ	0.04	6.39	<1	1/50
19	1.04	83	1.2	>10	45	2.3	2.9	1.46	36	1/50
22	1.72	73	8.2	>10	96	1.6	1.8	2.37	48	0/50
30	1.14	83	2.5	>10	82	2.3	0.8	2.72	74	3/50
35	-0.44	72	0.2	>10	65	0.22	0.02	13.9	<1	8/50
41	0.97	82	1.5	9.8	120	0.7	0.6	3.96	28	5/50
49	2.99	84	11.2	2.2	140	1.3	1.1	2.53	73	0/50

^aMeasured at pH 7.2. ^bApparent permeability in MDCK transwell culture, A:B apical to basolateral. ^c*In vitro* stability in cryopreserved rat hepatocytes. ^dNormalized to 5 mg/kg *po*, 1 mg/kg *iv*. ^eNumber of enzymes inhibited >50% out of a panel of 183 or 50 non-JAK kinases, at a test concentration of 100 × JAK1 K_i. ^fPlasma clearance following *iv* dosing. ^gPlasma area under the curve following *po* dosing. ^hMaximal plasma concentration following *po* dosing. ⁱVolume of distribution at steady state. ^jOral bioavailability. ^kData taken from ref ²⁶. ^lBelow the level of quantification.

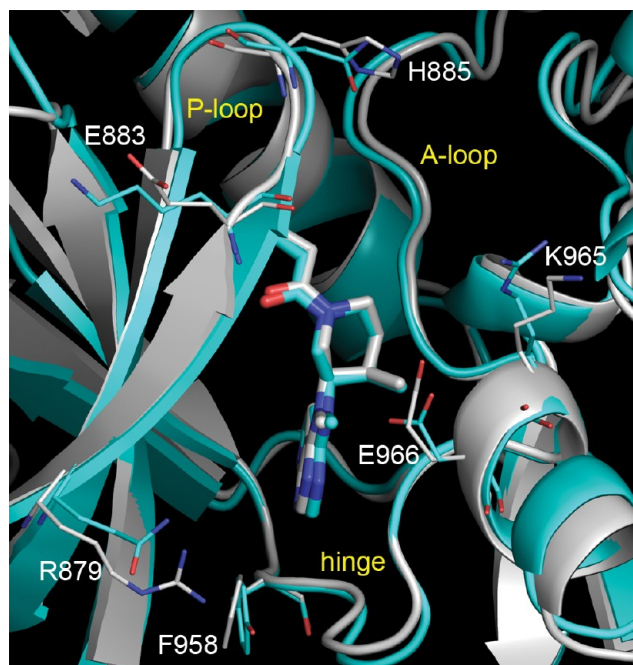


Figure 4. Comparison of the X-ray structures of **1** complexed with JAK1 (white carbon atoms; PDB ID 3EYG²⁷) and JAK2 (cyan carbon atoms; PDB ID 3FUP), showing the conserved binding mode of the ligand and the overall similarity in tertiary structure of the JAK isoforms. The phosphate-binding loop (P-loop), activation loop (A-loop), and hinge region are labeled. Residue differences between JAK1 and JAK2 that are located close to the ATP-binding site are shown in thin stick format. Residue numbers refer to JAK1. Figure was generated with Pymol.³⁸

degree of homology suggested that improvement of selectivity for JAK1 over JAK2 would not be a trivial task.³⁷

As desired in the original design, the binding mode of **1** is conserved in tricyclic analogue **7** (Figure 5). The pyrrolopyridine ring system of **7** binds to the hinge region (JAK1 residues Glu957 and Leu959) in a way similar to that of the pyrrolopyrimidine core of **1**. The piperidine ring binds to a small lipophilic pocket adjacent to Leu1010 (on the C-terminal wall), while the cyanoacetate group is directed deep under the P-loop. The nitrile does not form any direct hydrogen bonds but may make favorable electrostatic interactions with the

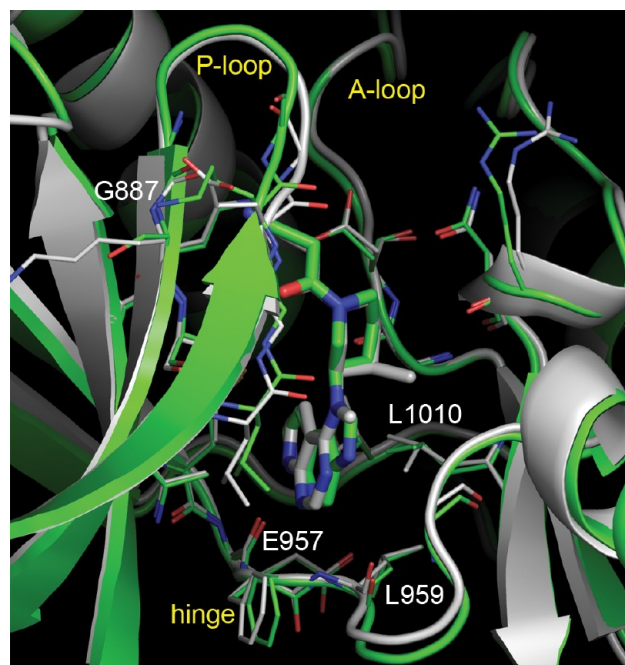


Figure 5. Comparison of the X-ray structures of **1** complexed with JAK1 (white carbon atoms; PDB ID 3EYG²⁷) and **7** complexed with a JAK2 triple mutant (green carbon atoms) showing the conserved binding mode. The phosphate-binding loop (P-loop), activation loop (A-loop), and hinge region are labeled. Residue numbers refer to JAK1. Figure generated with Pymol.³⁸

peptide backbone of the P-loop (e.g., the carbonyl carbon of Gly887) and the catalytic Lys908. The tight contacts of this group under the P-loop may explain the loss of potency for bulkier groups in this position on the 3-piperidine core (e.g., **8**). Transfer of the cyanoacetate to the 4-piperidine core (**15**) results in a loss of activity: molecular modeling studies suggest the acetonitrile group of **15** points along a different vector compared to **7** and hence is unable to bind as tightly under the P-loop.

In general, crystallographic studies revealed that small *N*-substituents on the 4-piperidinyl core sit loosely between the P-loop and the C-terminal lobe, close to residues associated with the binding of the phosphate of ATP, such as Asn1008 and

Asp1021 in JAK1. Larger substituents on the 4-piperidinyl, such as the benzyl group of **12**, were observed to be oriented toward the P-loop but caused some displacement of the P-loop compared with **1** and **7** (Figure 6). The observation that

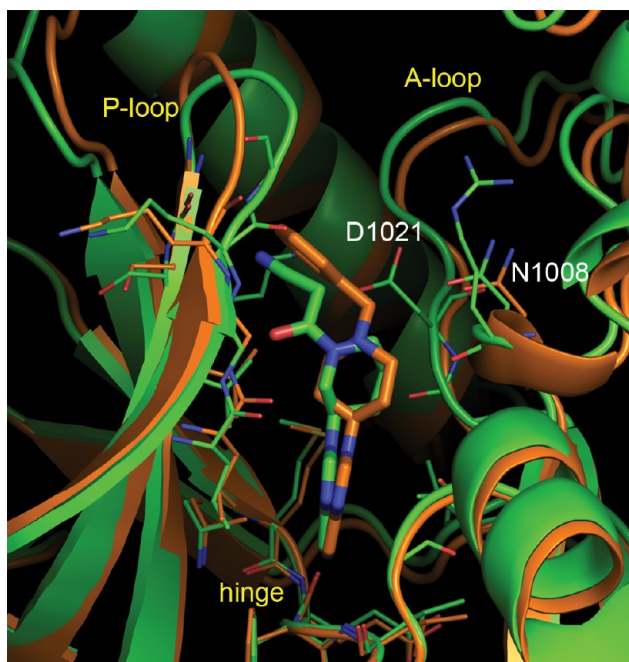


Figure 6. Comparison of the X-ray structures of **7** (green carbon atoms) and **12** (orange carbon atoms), both complexed with a JAK2 triple mutant, highlighting movement of the P-loop to accommodate the benzyl substituent of **12**. Residue labels refer to JAK1 numbering.

N-substituents on the 4-piperidine are bound loosely along the relatively spacious cleft between the P-loop and the C-terminal lobe may explain why a fairly wide range of substituents is tolerated at this position (Table 2).

N-Substitution of the 4-piperidine core with acetylamino groups (**23–27**) results in a general decrease in inhibitory activity for JAK1 but a gain in selectivity over JAK2. These groups are observed crystallographically to extend toward the bulk solvent between the edge of the P-loop and the C-terminal lobe. The SAR of these basic substituents may be modulated by electrostatic interactions with neighboring residues on the surface of the protein. The presence of several basic amino acids in this region on the C-terminal lobe (e.g., JAK1 Lys965, Arg1007) may impair the JAK1 potency of **23–27** due to electrostatic repulsion: the guanidine group of Arg1007 is located approximately 5 Å from the pyrrolidine nitrogen of **26**. Computational modeling studies (described in the Supporting Information) were used to compare the binding of **26** to JAK1 and several single residue mutants of JAK1 mimicking the corresponding residue changes in JAK2. These calculations suggested that the residue difference between Glu883 (JAK1) and Lys857 (JAK2) may drive the selectivity of **26** and similar molecules for JAK1 over JAK2. A visual comparison of the vacuum electrostatic potential of JAK1 to that of the *in silico* JAK1-E883K mutant illustrates this distinction: the increased positive electrostatic potential in the mutant is repulsive toward the positively charged pyrrolidine moiety on **26** (Figure 7). This is also consistent with the observation that other basic analogues, similar to **26**, are disfavored to a greater extent in JAK2 than in JAK1.

Methylation at the 4-position of the 4-piperidinyl group (Table 3) may have an effect on the SAR either by a direct interaction with the protein or by stabilization of the ligand conformation. The piperidinyl group is capable of adopting several low energy conformations with respect to the tricyclic core, due to rotation around the bond between the piperidine and the imidazo ring of the tricycle. In X-ray structures of 3-piperidinyl analogues, including **1**, the hydrogen atom at the 3-position of the piperidinyl moiety (i.e., that on the carbon atom at the point of attachment of the piperidinyl ring to the tricycle) is directed toward the pyrrolo ring of the hinge binder; this conformation allows the *N*-substituent to be directed under the

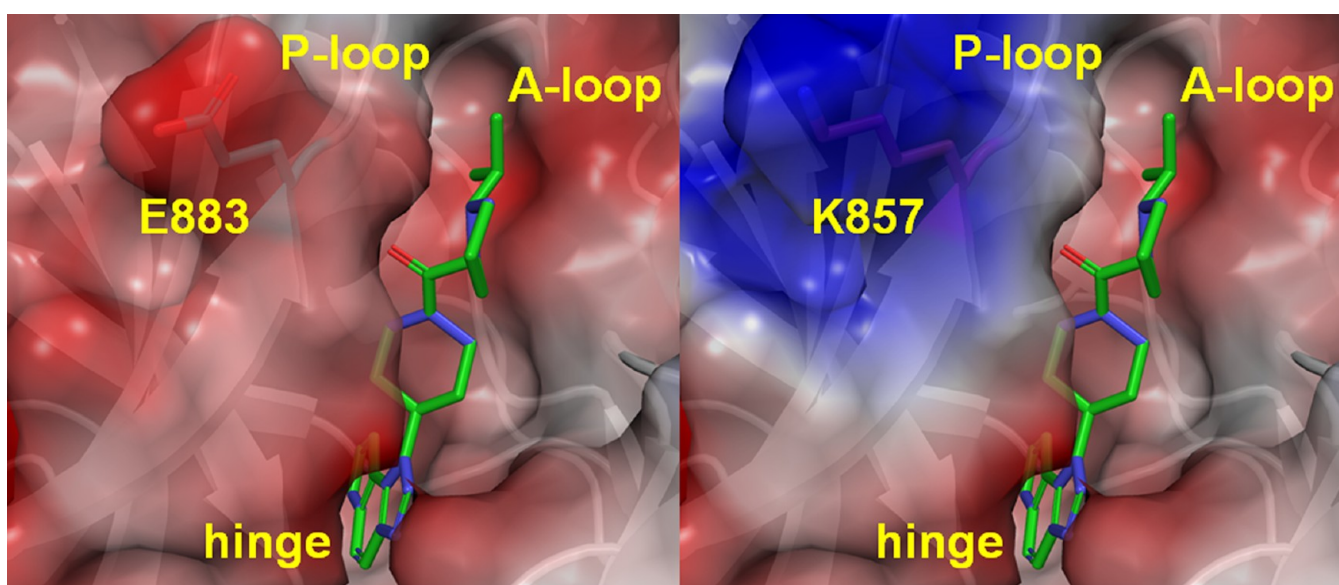


Figure 7. Electrostatic potential representations for the X-ray structure of **26** bound to JAK1 (left) and an *in silico* model of **26** bound to a JAK1-E883K mutant (right). Ligands are displayed in stick format with green carbon atoms. Surfaces colored by electrostatic potential from red (negative) to blue (positive). A similar orientation of each protein is shown. Surfaces and images were generated with Pymol's protein contact potential algorithm which approximates the potential that would be felt by a point-charge one solvent radius above the protein surface (Schrödinger, Inc.).

P-loop. In the 4-piperidinyl series, a broader range of piperidine rotamers is observed crystallographically, presumably influenced to some extent by the binding interactions of substituents on the piperidinyl ring. Thus, methylation on the 4-position may serve to stabilize or destabilize specific conformations of the piperidine (e.g., due to steric interactions with the pyrrolo ring of the hinge binder) and thereby influence the binding interactions of substituents on the piperidinyl ring, as well as modulate direct lipophilic contacts between the piperidinyl ring and the C-terminal wall (e.g., Leu1010) (Figure 8).

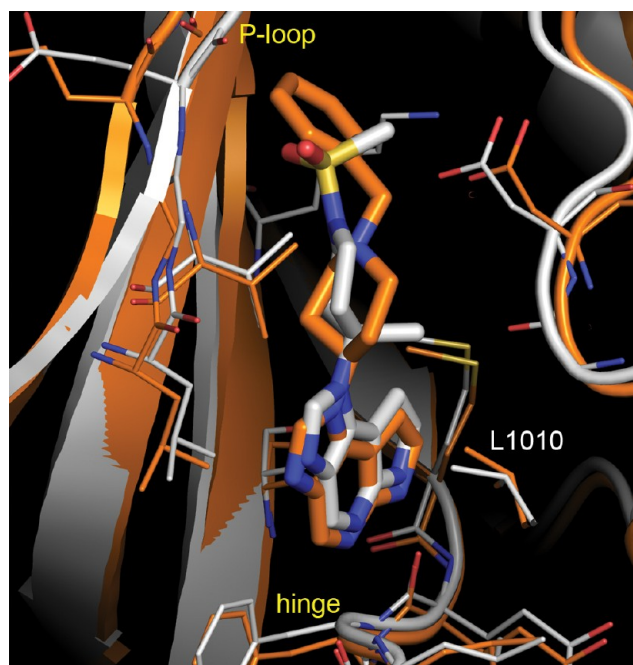


Figure 8. Comparison of the X-ray structures of **12** in JAK2 triple mutant (orange carbon atoms) and **30** in JAK1 (white carbon atoms), highlighting different piperidine rotamers due to 4-methylation in **30**.

X-ray structures also revealed that the piperidinyl ring of **30** adopted different rotamers when bound in JAK1 and JAK2; the latter was associated with significant movement of the P-loop into the binding site in order to maximize contacts with the inhibitor (Figure 9). This difference in protein conformation may be an experimental artifact, possibly due to crystal packing contacts which were present in JAK2 but absent in JAK1; it was also noted that the electron density for the P-loop was less complete for the JAK1 complex. The significant shift in the ligand binding mode might have been expected to result in a much greater difference in potency between JAK1 and JAK2, and was not observed for similar inhibitors. However, it is also worth noting that there are several residue differences between JAK1 and JAK2 along the P-loop; although these side chains are directed away from the ligand-binding site, it is possible that they may affect the flexibility of the P-loop such that different low-energy conformations may be accessed by JAK1 compared with JAK2.

In general, compounds in the cyclohexyl and cyclopentyl series (Table 4) were observed to bind similarly to the piperidinyl series. As may be expected, substituents on the cyclopentyl ring are directed along a vector intermediate between the vectors presented by the 3-piperidinyl and the 4-piperidinyl rings, and hence may show somewhat different trends in SAR. For example, the relatively bulky carbamate substituent of **49** lies along the groove between

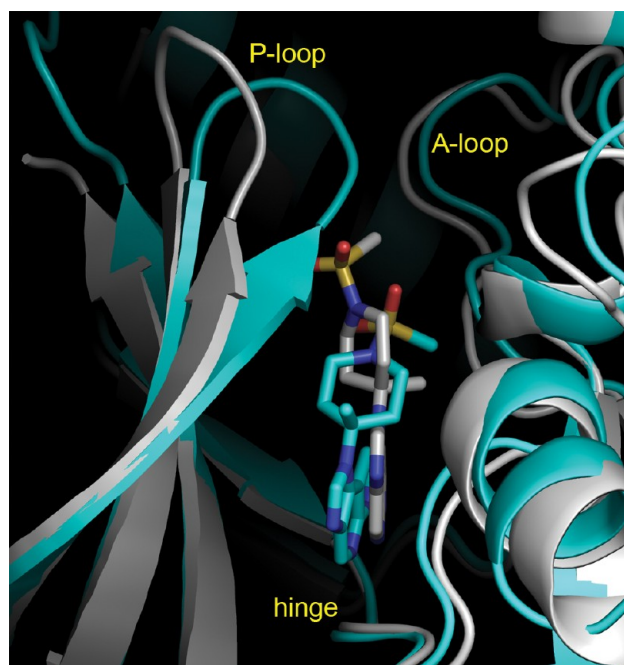


Figure 9. Comparison of the X-ray structures of **30** bound to JAK1 (white carbon atoms) and JAK2 (cyan carbon atoms), highlighting a shift in the binding mode and significant movement of the P-loop.

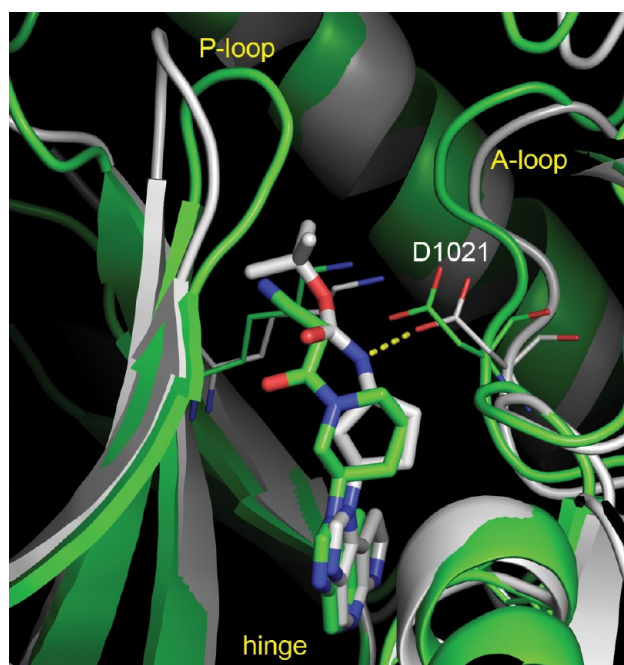
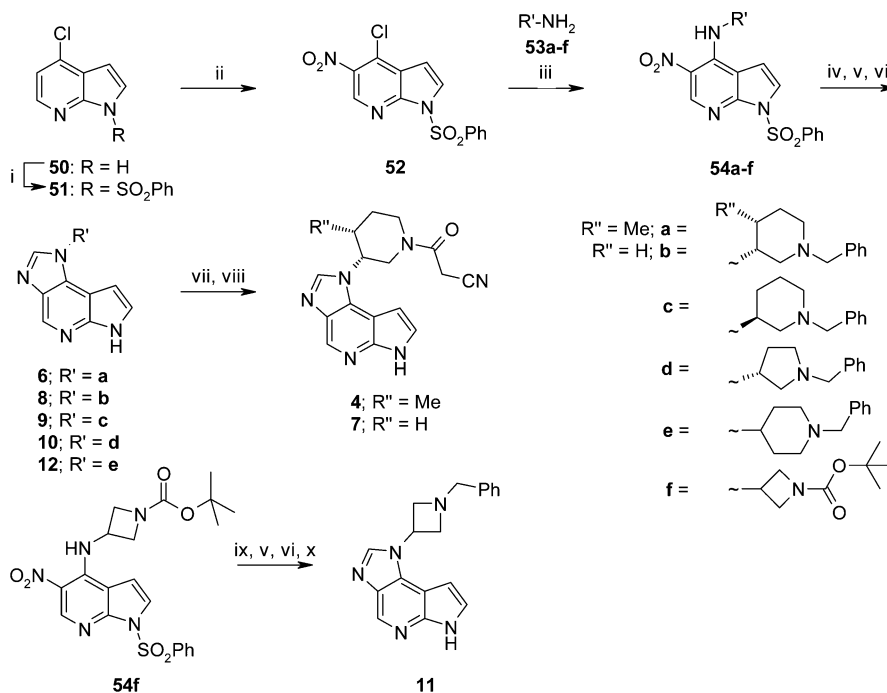


Figure 10. Comparison of the X-ray structures of **7** bound to JAK2 triple mutant (green carbon atoms) and **49** bound to JAK1 (white carbon atoms) to demonstrate the different vectors adopted by the substituents on the 3-piperidinyl and cyclopentyl rings, respectively. A potential hydrogen bond is highlighted between **49** and D1021 (yellow dotted line).

the P-loop and the C-terminal wall, forming a single direct hydrogen bond to the protein to Asp1021 (Figure 10).

CHEMISTRY

Protection of 4-chloro-7-azaindole **50**³⁹ with benzenesulfonyl chloride provided **51** (Scheme 1), which was regioselectively nitrated at the 5-position using tetrabutylammonium nitrate in

Scheme 1. Preparation of Heterocycloamine Derivatives of 3^a

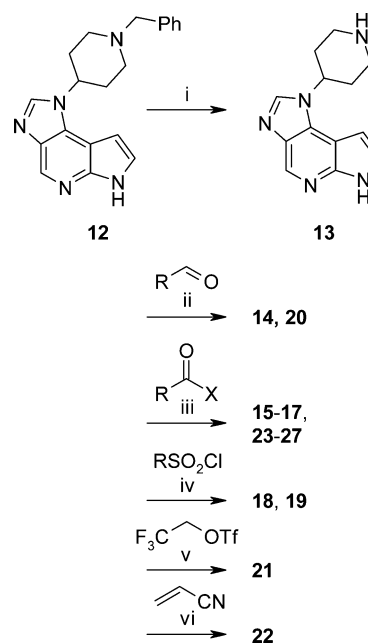
^aReagents and conditions: (i) PhSO₂Cl, DMAP (cat.), NEt₃, DCM, rt, overnight, 83%; (ii) *n*-Bu₄N⁺NO₃⁻, TFAA, DCM, -5 °C-rt, overnight, 79%; (iii) R'NH₂, EtN(*i*-Pr)₂, *i*-PrOH, 120 °C in microwave, 11–20 min, 80–100%; (iv) Fe, NH₄Cl, EtOH, H₂O, reflux, 70–99%; (v) (EtO)₃CH, *p*-TsOH (cat.), PhMe, reflux, 18 h, 81–100%; (vi) NaOH, MeOH, H₂O, rt, 7 h, 72–98%; (vii) Pd(OH)₂ on C, NH₄HCO₂, MeOH, reflux; (viii) NCCH₂CO₂H, HOBT, DMAP, EDCl, DCM, rt, 24 h, 11–48% 2 steps; (ix) Pd on C, H₂, THF; (x) TFA, DCM, 94%, then PhCHO, Na(OAc)₃BH, AcOH, DCE, MeOH, rt, 91%.

the presence of trifluoroacetic anhydride.⁴⁰ S_NAr displacement of chloride in key intermediate **52** with amines **53a–f** afforded **54a–f**. Amine **53a** was prepared according to the published procedure.⁴¹ Iron-mediated reduction⁴² followed by cyclization proceeded uneventfully, and the product was deprotected under basic conditions to give the compounds shown in Table 1 (**6**, **8–10**, and **12**). In the case of azetidine **11**, the precursor *t*-butyl carbamate was deprotected using TFA and the resulting secondary amine reductively alkylated with benzaldehyde. Transfer hydrogenolysis of the *N*-benzyl groups of **6** and **8**, with subsequent cyanoacetylation provided **4** and **7**, respectively.

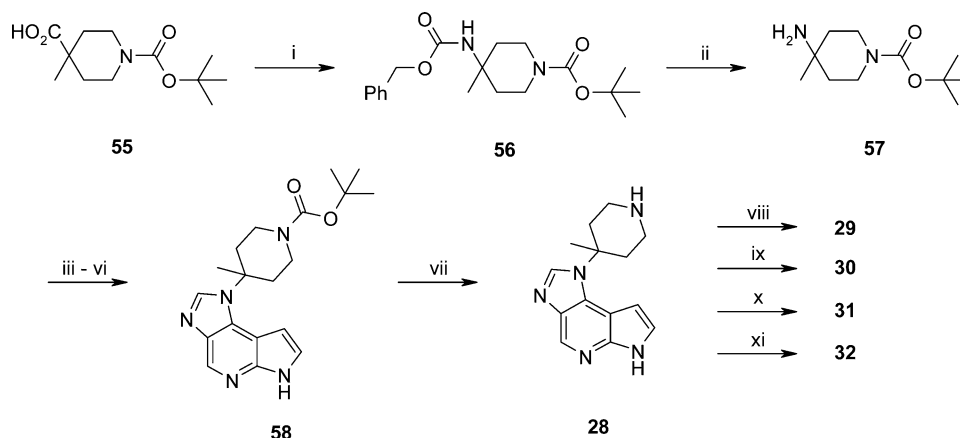
Hydrogenolysis of **12** provided **13**, which was derivatized under standard conditions (Scheme 2) to give the compounds in Table 2.

Piperidine derivatives bearing a 4-methyl group were prepared in accordance with the sequence depicted in Scheme 3. Curtius rearrangement of commercially available Boc-protected piperidine carboxylate **55** in the presence of benzyl alcohol afforded bis carbamate **56**. Selective deprotection gave amine **57**, which required significantly more forcing conditions than those employed previously to react with **52** on account of its hindered nature. Manipulation of the adduct in a manner analogous to that described above gave **58**, which on deprotection furnished **28**. Derivatization of the piperidine provided the other compounds listed in Table 3.

Synthesis of cyclohexylamine derivatives **33**, **35**, and **39–45** followed an analogous process (Scheme 4), starting with monoprotected *trans*-cyclohexyl-1,4-diamine **59**. Compounds **34** and **36** were prepared in a fashion corresponding to that of **33** and **35**, respectively, only using the *cis* diastereomer of **59**.

Scheme 2. Preparation of 4-Piperidinyl Analogues^a

^aReagents and conditions: (i) Pd(OH)₂ on C, NH₄HCO₂, MeOH, reflux, 52%; (ii) Na(OAc)₃BH, AcOH, DCE, MeOH, rt, 57–68%; (iii) **15**, **16**, X = OH HOBT, DMAP, EDCl, DCM, rt, 32–57%; **17**, X = Cl NEt₃, DCM, rt, 52%; **23**, **25–27**, X = OH HATU, EtN(*i*-Pr)₂, DMF; **24**, then TFA, DCM, then HCHO, Na(OAc)₃BH, AcOH, DCE; (iv) EtN(*i*-Pr)₂, DMF, THF, 13–18%; (v) NEt₃, DCM, DMF, rt, 46%; (vi) EtOH, reflux, 87%.

Scheme 3. Preparation of 4-Methyl Piperidinyl Analogues^a

^aReagents and conditions: (i) $\text{Ph}_2\text{P}(\text{O})\text{N}_3$, NEt_3 , PhCH_2OH , PhMe , reflux; (ii) Pd on C, H_2 , EtOH, 47% 2 steps; (iii) **52**, $\text{EtN}(i\text{-Pr})_2$, $i\text{-PrOH}$, reflux, 65 h, 79%; (iv) Fe, NH_4Cl , MeOH, H_2O , reflux, 84%; (v) $(\text{EtO})_3\text{CH}$, $p\text{-TsOH}$ (cat.), PhMe , reflux, 86%; (vi) NaOH, MeOH, H_2O , rt, 98%; (vii) TFA, DCM, rt, 98%; (viii) pyrimidine-5-carboxaldehyde, $\text{Na}(\text{OAc})_3\text{BH}$, AcOH, mol. sieves, DCE, rt, 47%; (ix) MeSO_2Cl , NEt_3 , DCM, rt, 58%; (x) $\text{TfOCH}_2\text{CF}_3$, NEt_3 , DCM, DMF, rt, 87%; (xi) acrylonitrile, EtOH, reflux, 57%.

Morpholine derivatives **37** and **38** were prepared (Scheme 5) by reductive amination of cyclohexanone **65** with morpholine, followed by separation of diastereomers **66** and subsequent deprotection. Compound **65** arose through oxidation of alcohol **64**, itself obtained through a process analogous to that described previously, starting with amino alcohol **63**,

The preparation of cyclopentylamine derivatives **47–49** is described in Scheme 6. Palladium-mediated reduction of bicyclic hydroxylamine **67**⁴³ followed by N–O bond cleavage with Raney nickel⁴⁴ afforded protected *cis* amino alcohol **68**. Mesylation, azide displacement⁴⁵ and subsequent reduction gave *trans* diamine derivative **70**. This was progressed as previously described to sulfonyl-protected tricycle **72**, which gave **47** on basic hydrolysis. This was subjected to SFC resolution, giving **49** as the more active enantiomer. Conversely, **73** was prepared by sequential reaction of **72** with TFA and methyl chloroformate, followed by hydrolysis as before to **46**. The *cis*-diastereomer **48** was synthesized in a manner analogous to that for **47**, following Mitsunobu inversion of **68** to **69**.⁴⁶

CONCLUSIONS

Taking account of reported clinical experience with pan-JAK inhibitors and the important role of IL-6 in mediating inflammatory response, it was postulated that selective modulation of the JAK1 signaling pathway represented a valid strategy for the potential treatment of pro-inflammatory conditions such as RA. A significant, recent increase in patent applications claiming kinase inhibitors with selectivity for the JAK1 isoform would suggest this to be an emerging area of interest.

A novel, imidazo-pyrrolopyridine hinge-binding scaffold was identified which appeared to possess an innate preference for JAK1 over the other JAK isoforms. While the selectivities quoted are undeniably subtle, they are nonetheless consistent, with virtually all of the compounds within this series showing some degree of JAK1 preference, in contrast to the structurally related, bicyclic inhibitor **1**. Since such a profile was unexpected, attention was taken to ensure accuracy of reported data. As noted elsewhere, all quoted biochemical and cellular data are the mean of at least three separate experiments; furthermore, on average, the coefficient of variation was less than 0.35 and 0.5 times the mean for biochemical and cell

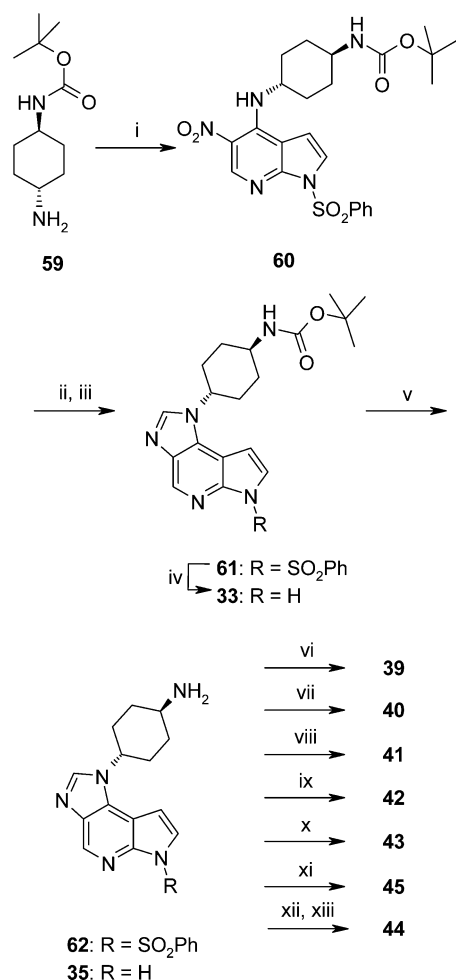
assays, respectively. Moreover, good agreement was generally observed between the selectivity in both biochemical and cellular assays for any given compound. A further feature of this series was the excellent JAK1 inhibitory activity displayed by the majority of examples. The accommodation of a wide variety of chemotypes allowed for ready modulation of physicochemical properties, thereby providing the means for achieving good correlation between biochemical and cell potencies, and favorable rat pharmacokinetic characteristics.

X-ray crystallography proved valuable for confirming the general binding mode of the series and also demonstrated the subtle differences in binding contacts achievable by changes to substitution patterns. In particular, structural information was useful in guiding the design of analogues toward regions of the protein that may be expected to yield improvements in affinity and selectivity. Further optimization of this series, particularly with regard to improving selectivity and demonstrating *in vivo* activity in a relevant model of inflammatory disease, will be disclosed elsewhere.

EXPERIMENTAL SECTION

General Methods. Commercial reagents and solvents were used as supplied. Use of ethanol as reaction solvent refers to industrial methylated spirit. Moisture or oxygen sensitive reactions were conducted under an atmosphere of argon or nitrogen gas. Chemical and optical (where applicable) purities were >95% for all final compounds as assessed by quantitative HPLC with DAD UV detection and chiral SFC analysis, respectively. Further details on the analytical conditions used for individual compounds may be found in Supporting Information. ¹H NMR spectra were recorded at ambient temperature using Varian Unity Inova or Bruker Avance DRX400 instruments operating at the indicated frequencies. Chemical shifts were expressed in ppm relative to an internal standard, tetramethylsilane (ppm = 0.00). The following abbreviations were used: br = broad signal, s = singlet, d = doublet, dd = doublet of doublets, t = triplet, q = quartet, p = pentet, and m = multiplet. Microwave experiments were carried out using a Biotage Initiator 2.0 (400 W MAGNETRON) which uses a single-mode resonator and dynamic field tuning.

Strong cation exchange chromatography was performed using Biotage Isololute SCX-2 columns. Silica gel chromatography was performed using medium-pressure liquid chromatography (MPLC) on a CombiFlash Companion (Teledyne Isco) with RediSep normal phase silica gel (35–60 μm) columns and UV detection at 254 nm.

Scheme 4. Preparation of 4-Cyclohexylamine Analogues^a

^aReagents and conditions: (i) 52, EtN(*i*-Pr)₂, *i*-PrOH, reflux, 1 h, 80%; (ii) Fe, NH₄Cl, MeOH, H₂O, reflux, 80%; (iii) (EtO)₃CH, *p*-TsOH (cat.), PhMe, reflux, 88%; (iv) NaOH, MeOH, THF, rt, 81%; (v) TFA, DCM, rt, 1 h, 95%; (vi) 62, isobutyl chloride, EtN(*i*-Pr)₂, DMAP, DCM, rt, then NaOH, MeOH, rt, 30%; (vii) 62, cyclopropylcarboxaldehyde, Na(OAc)₃BH, MeOH, rt, then NaOH, MeOH, rt, 44%; (viii) 35, acrylonitrile, EtOH, reflux, 36%; (ix) 35, 3-cyanobenzaldehyde, Na(OAc)₃BH, AcOH, mol. sieves, DCE, rt, 24%; (x) 35, MeSO₂Cl, NEt₃, DCM, rt, 38%; (xi) 62, 4-nitrophenyl chloroformate, pyridine, 0 °C, then NaOMe, MeOH, 100 °C in microwave, 10 min, 24%; (xii) 62, Ac₂O, HCO₂H, THF, then BH₃-THF, THF, 80 °C 86%; (xiii) methyl chloroformate, EtN(*i*-Pr)₂, DCM, then NaOH, THF, MeOH, H₂O, rt, 55%.

Reverse phase high performance liquid chromatography (HPLC) was used to purify compounds where indicated. Unless otherwise indicated, the conditions were elution on a Phenomenex Gemini C18 column (250 × 21.2 mm, 5 μm) as stationary phase and using mobile phase indicated, operating at a 18 mL/min flow rate using a Gilson UV/vis -155 dual channel detector and Gilson GX-271 automated liquid handler.

JAK Enzyme Assays. The activity of the isolated JAK1, JAK2, or TYK2 kinase domain was measured by monitoring the phosphorylation of a peptide derived from JAK3 (Val-Ala-Leu-Val-Asp-Gly-Tyr-Phe-Arg-Leu-Thr-Thr) fluorescently labeled on the N-terminus with 5-carboxyfluorescein using the Caliper LabChip technology (Caliper Life Sciences, Hopkinton, MA). Alternatively, the activity of the isolated JAK3 kinase domain was measured by monitoring the phosphorylation of a different peptide derived from JAK3 (Leu-Pro-Leu-Asp-Lys-Asp-Tyr-Tyr-Val-Val-Arg) fluorescently labeled on the

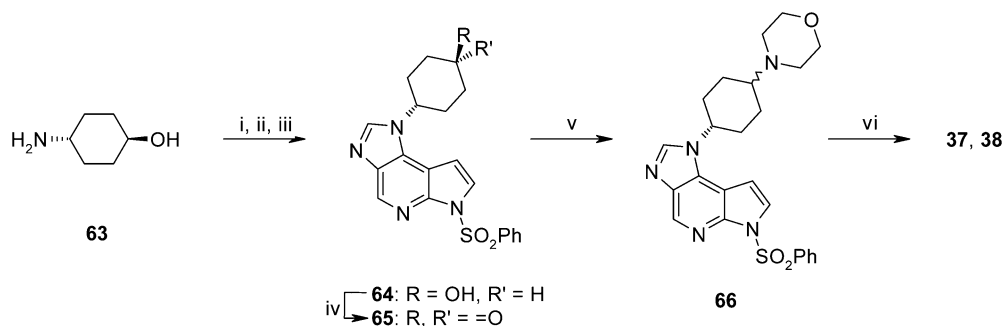
N-terminus with 5-carboxyfluorescein using the same Caliper LabChip technology. To determine inhibition constants (*K_i*), compounds were diluted serially in DMSO and added to 50 μL kinase reactions containing 1.5 nM purified JAK1, 0.2 nM purified JAK2, 5 nM purified JAK3, or 1 nM purified TYK2 enzyme, 100 mM HEPES buffer (pH 7.2), 0.015% Brij-35, 1.5 μM peptide substrate, 25 μM ATP (5 μM ATP in the case of JAK3), 10 mM MgCl₂, and 4 mM DTT at a final DMSO concentration of 2%. Reactions were incubated at 22 °C in 384-well polypropylene microtiter plates for 30 min and then stopped by the addition of 25 μL of an EDTA containing solution (100 mM HEPES buffer pH 7.2, 0.015% Brij-35, 150 mM EDTA), resulting in a final EDTA concentration of 50 mM. After termination of the kinase reaction, the proportion of phosphorylated product was determined as a fraction of total peptide substrate using the Caliper LabChip 3000 according to the manufacturer's specifications. *K_i* values were then determined using the Morrison tight binding model.⁴⁷

JAK Cellular Assays. The activities of compounds were determined in cell-based assays that are designed to measure JAK-dependent STAT phosphorylation. TF-1 cells were obtained from the American Type Culture Collection (ATCC; Manassas, VA). TF-1 cells were starved overnight in OptiMEM medium with 0.5% Charcoal/Dextran stripped fetal bovine serum (FBS), 0.1 mM nonessential amino acids (NEAA), 1 mM sodium pyruvate, and without phenol red at 37 °C. Compounds were serially diluted in DMSO and incubated for 20 min at 37 °C with TF-1 cells in 384-well microtiter plates in RPMI-1640 at a final cell density of 100,000 cells per well and a final DMSO concentration of 0.2%. Human recombinant cytokines, IL-6 (30 ng/mL), or EPO (10 U/mL) were then added at the final concentrations indicated to the microtiter plates containing the TF-1 cells, and compound and the plates were incubated for 30–45 min at 37 °C. Compound-mediated effects on STAT3 (IL-6) or STAT5 (EPO) phosphorylation were then measured in the lysates of cells using the Meso Scale Discovery (MSD) technology (Gaithersburg, Maryland) according to the manufacturer's protocol. EC₅₀ values were determined as the concentration of compound required for 50% inhibition of STAT phosphorylation relative to that measured for the DMSO control.

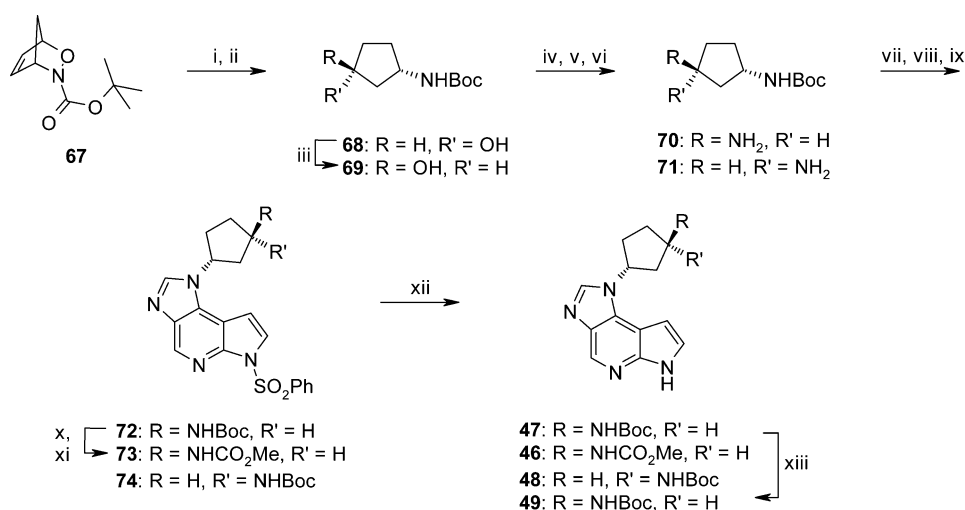
4-Chloro-1-phenylsulfonyl-1H-pyrrolo[2,3-*b*]pyridine (51). A stirred suspension of 4-chloro-7-azaindole (50; 1.00 g, 6.55 mmol) in (DCM) 50 mL was treated with DMAP (80.0 mg, 0.66 mmol), triethylamine (1.36 mL, 9.83 mmol), and benzenesulfonyl chloride (0.93 mL, 7.21 mmol) at ambient temperature. The mixture was left to stand overnight. After dilution with DCM, the reaction mixture was washed with 1 M aqueous HCl solution, saturated sodium hydrogen carbonate solution, water, and brine, dried with sodium sulfate, and concentrated under vacuum to give a brown solid. Trituration (diethyl ether) afforded 1.59 g (83%) of 51 as a beige solid. LCMS (Method 2, ESI): RT = 4.48 min, m+H = 293.3. ¹H NMR (400 MHz, CDCl₃) δ: 8.31 (d, *J* = 5.3 Hz, 1 H), 8.18 (m, 2 H), 7.8 (d, *J* = 4.1 Hz, 1 H), 7.58 (m, 1 H), 7.49 (m, 1 H), 7.20 (d, *J* = 5.3 Hz, 1 H), 6.71 (d, *J* = 4.1 Hz, 1 H).

4-Chloro-5-nitro-1-phenylsulfonyl-1H-pyrrolo[2,3-*b*]pyridine (52). Tetrabutylammonium nitrate (381 mg, 1.25 mmol) dissolved in DCM (5 mL) was added dropwise to a stirred solution of 51 (293 mg, 1.00 mmol) in DCM (5 mL) at -5 °C. Trifluoroacetic anhydride (180 μL, 1.29 mmol) was added while maintaining the reaction temperature below 0 °C. The mixture was then stirred at -5 °C for 30 min and ambient temperature for 5 h. TLC indicated incomplete reaction; therefore, 0.25 equiv each of tetrabutylammonium nitrate and trifluoroacetic anhydride were added and the resulting mixture left to stand for 18 h at ambient temperature. DCM was added, and the mixture washed with water, dried with sodium sulfate, and concentrated under vacuum to give a yellow solid. Purification by column chromatography on silica gel (gradient: 0 to 25% ethyl acetate in cyclohexane) gave 266 mg (79%) of 52 as a white solid. LCMS (Method 2, ESI): RT = 4.57 min, m+H = 338.4. ¹H NMR (400 MHz, CDCl₃) δ: 9.00 (s, 1 H), 8.21 (m, 2 H), 7.94 (d, *J* = 4.1 Hz, 1 H), 7.66 (t, *J* = 7.5 Hz, 1 H), 7.55 (t, *J* = 7.8 Hz, 2 H), 6.87 (d, *J* = 4.1 Hz, 1 H).

(±)-*cis*-*N*-[4-Methyl-1-(phenylmethyl)-piperidin-3-yl]-5-nitro-1-(phenylsulfonyl)-1H-pyrrolo[2,3-*b*]pyridin-4-amine (54a). A mixture of 52 (692 mg, 2.05 mmol), (±)-*cis*-4-methyl-1-(phenylmethyl)-piperidin-3-ylamine (460 mg, 2.25 mmol), and *N,N*-diisopropylethylamine

Scheme 5. Preparation of Morpholine Derivatives 37 and 38^a

^aReagents and conditions: (i) **52**, EtN(*i*-Pr)₂, *i*-PrOH, reflux, 2 h, quant.; (ii) Fe, NH₄Cl, EtOH, H₂O, reflux, 2 h, 52%; (iii) (EtO)₃CH, AcOH, 110 °C, 0.25 h, then rt, 82%; (iv) Dess–Martin periodinane, DCM, 0 °C–rt, 89%; (v) morpholine, Na(OAc)₃BH, AcOH, THF, rt, 20 h, then chromatographic separation, *trans*: 19%, *cis*: 23%; (vi) NaOH, MeOH, H₂O, *trans*, 67%.

Scheme 6. Preparation of Cyclopentylamine Analogues^a

^aReagents and conditions: (i) Pd on C, H₂, EtOH, 97%; (ii) Raney Ni, H₂, EtOH, 75%; (iii) diisopropyl azodicarboxylate, PPh₃, AcOH, THF, 0 °C–rt, then NaOH, MeOH, THF, H₂O, rt, 76% 2 steps; (iv) MsCl, Et₃N, acetone, 0 °C, 98%; (v) NaN₃, DMF, H₂O, 100 °C, 77–97%; (vi) PPh₃, THF, H₂O, 55 °C, 87–91%; (vii) **52**, EtN(*i*-Pr)₂, *i*-PrOH, 120 °C in microwave, 10 min, 87%–quant.; (viii) Fe, NH₄Cl, EtOH, H₂O, reflux, 70%; (ix) (EtO)₃CH, *p*-TsOH (cat.), PhMe, reflux, 77%; (x) TFA, DCM, rt, 86%; (xi) MeO₂CCL, EtN(*i*-Pr)₂, DCM, quant.; (xii) NaOH, THF, MeOH, H₂O, 89%; (xiii) SFC resolution.

(1.25 mL, 7.2 mmol) in 2-propanol was heated at 95 °C for 2 h. The reaction mixture was cooled, and the yellow precipitate that formed was isolated by filtration and dried *in vacuo* to afford 940 mg (90%) of **54a**. LCMS (Method 3, ESI): RT = 2.61 min, m+H = 506.2.

(±)-*cis*-1-[4-Methyl-1-(phenylmethyl)-piperidin-3-yl]-1,6-dihydro-imidazo[4,5-*d*]pyrrolo[2,3-*b*]pyridine (**6**). *Step 1*: (±)-*cis*-*N*^t-[4-Methyl-1-(phenylmethyl)-piperidin-3-yl]-1-(phenylsulfonyl)-1*H*-pyrrolo[2,3-*b*]pyridine-4,5-diamine. A mixture of **54a** (940 mg, 1.86 mmol), iron powder (~325 mesh, 415 mg, 7.44 mmol), and ammonium chloride (597 mg, 11.16 mmol) in a methanol/water mixture (3:1, 64 mL) was heated at reflux for 4 h. The cooled mixture was filtered through Celite and washed with methanol. The filtrate was concentrated under vacuum and the residue obtained partitioned between saturated aqueous sodium bicarbonate and DCM. The aqueous phase was extracted twice with DCM. The combined extracts were washed with brine, dried (sodium sulfate), and concentrated under vacuum. Purification by column chromatography on silica gel (gradient: 0 to 5% [2 M ammonia in methanol] in DCM) afforded 620 mg (70%) of (±)-*cis*-*N*^t-[4-methyl-1-(phenylmethyl)-piperidin-3-yl]-1-(phenylsulfonyl)-1*H*-pyrrolo[2,3-*b*]pyridine-4,5-diamine as a white foam. LCMS (Method 3, ESI): RT = 2.16 min, m+H = 476.1.

Step 2: (±)-*cis*-1-[4-Methyl-1-(phenylmethyl)-piperidin-3-yl]-6-(phenylsulfonyl)-1,6-dihydro-imidazo[4,5-*d*]pyrrolo[2,3-*b*]pyridine. A mixture of (±)-*cis*-*N*^t-[4-methyl-1-(phenylmethyl)-piperidin-3-yl]-1-

(phenylsulfonyl)-1*H*-pyrrolo[2,3-*b*]pyridine-4,5-diamine (420 mg, 0.90 mmol), triethyl orthoformate (375 μL, 2.25 mmol), and *p*-toluenesulfonic acid monohydrate (17.0 mg, 90 μmol) in toluene (25 mL) was heated at reflux for 16 h. After cooling, ethyl acetate was added and the mixture washed with saturated aqueous sodium hydrogen carbonate, water and brine, dried with sodium sulfate, and concentrated under vacuum. Purification by column chromatography on silica gel (gradient: 0 to 4% [2 M ammonia in methanol] in DCM) afforded 356 mg (81%) of (±)-*cis*-1-[4-methyl-1-(phenylmethyl)-piperidin-3-yl]-6-(phenylsulfonyl)-1,6-dihydro-imidazo[4,5-*d*]pyrrolo[2,3-*b*]pyridine as a white foam. LCMS (Method 3, ESI): RT = 2.61 min, m+H = 486.1.

Step 3: (±)-*cis*-1-[4-Methyl-1-(phenylmethyl)-piperidin-3-yl]-1,6-dihydro-imidazo[4,5-*d*]pyrrolo[2,3-*b*]pyridine (**6**). A mixture of (±)-*cis*-1-[4-methyl-1-(phenylmethyl)-piperidin-3-yl]-6-(phenylsulfonyl)-1,6-dihydro-imidazo[4,5-*d*]pyrrolo[2,3-*b*]pyridine (356 mg, 0.73 mmol) and 1 M aqueous sodium hydroxide (3.65 mL, 3.65 mmol) in methanol/THF was stirred at room temperature for 64 h. The reaction mixture was concentrated under vacuum, and the residue obtained partitioned between saturated sodium bicarbonate solution and DCM. The aqueous phase was extracted twice with DCM. The combined extracts were washed with brine, dried (sodium sulfate), and concentrated under vacuum to afford 223 mg (89%) of **6** as a cream colored

foam. LCMS (Method 1, ESI): RT 2.39 min, m+H = 346.3. ¹H NMR (400 MHz, DMSO-*d*₆) δ: 11.78 (s, 1 H), 8.91 (s, 1 H), 8.56 (s, 1 H), 7.42 (t, *J* = 3.0 Hz, 1 H), 7.32–7.34 (m, 4 H), 7.22–7.24 (m, 1 H), 6.87 (dd, *J* = 3.4, 1.9 Hz, 1 H), 5.04 (d, *J* = 4.0 Hz, 1 H), 3.56–3.57 (m, 2 H), 3.02–3.06 (m, 2 H), 2.63 (dd, *J* = 12.1, 3.2 Hz, 1 H), 2.16–2.22 (m, 2 H), 1.53–1.61 (m, 2 H), 0.54 (d, *J* = 6.8 Hz, 3 H).

(±)-cis-3-(Imidazo[4,5-*d*]pyrrolo[2,3-*b*]pyridin-1(6*H*)-yl)-4-methylpiperidin-1-yl)-3-oxopropanenitrile (4). *Step 1:* (±)-cis-1-(4-Methyl-piperidin-3-yl)-1,6-dihydro-imidazo[4,5-*d*]pyrrolo[2,3-*b*]pyridine. A mixture of **6** (180 mg, 0.52 mmol), palladium hydroxide (20 wt % on carbon, 37 mg, 0.05 mmol), and ammonium formate (328 mg, 5.2 mmol) in methanol was heated at 60 °C for 24 h. The cooled mixture was filtered through Celite and the filter cake washed with methanol. The filtrate was concentrated under vacuum to afford 110 mg (82%) of (±)-cis-1-(4-methyl-piperidin-3-yl)-1,6-dihydro-imidazo[4,5-*d*]pyrrolo[2,3-*b*]pyridine as an off-white solid. LCMS (Method 3, ESI): RT 0.35 min, m+H = 255.9.

Step 2: (±)-cis-3-(Imidazo[4,5-*d*]pyrrolo[2,3-*b*]pyridin-1(6*H*)-yl)-4-methylpiperidin-1-yl)-3-oxopropanenitrile (4). A mixture of (±)-cis-4-methyl-piperidin-3-yl)-1,6-dihydro-imidazo[4,5-*d*]pyrrolo[2,3-*b*]pyridine (110 mg, 0.43 mmol), cyanoacetic acid (40 mg, 0.47 mmol), HOBt (87 mg, 0.65 mmol), EDCI (167 mg, 0.86 mmol), and DMAP (105 mg, 0.86 mmol) in DCM was stirred at room temperature for 18 h. The reaction mixture was evaporated to dryness and purified by column chromatography on silica gel (gradient: 0 to 6% [2 M ammonia in methanol] in DCM) to give 43 mg (31%) of **4** as an off-white solid. Further purification by HPLC (gradient: 5–40% acetonitrile containing 0.1% v/v aqueous ammonia in 0.1% v/v aqueous ammonia) afforded 15 mg (11%) of **4** as a white solid. LCMS (Method 1, ESI): RT 2.14 min, m+H = 323.3. ¹H NMR (400 MHz, DMSO-*d*₆) δ: 11.85 (s, 1 H), 8.59–8.60 (m, 1 H), 8.23–8.59 (m, 1 H), 7.46 (t, *J* = 3.0 Hz, 1 H), 6.87–6.89 (m, 1 H), 5.08 (d, *J* = 4.7 Hz, 1 H), 4.38–4.40 (m, 2 H), 4.10 (d, *J* = 18.7 Hz, 1 H), 3.83 (d, *J* = 20.0 Hz, 1 H), 3.72 (d, *J* = 14.7 Hz, 1 H), 3.60 (dd, *J* = 13.8, 3.61 Hz, 1 H), 2.42 (br s, 1 H), 1.71–1.77 (m, 2 H), 0.64 (dd, *J* = 23.1, 6.83 Hz, 3 H).

N-[1-(Phenylmethyl)-piperidin-4-yl]-5-nitro-1-(phenylsulfonyl)-1*H*-pyrrolo[2,3-*b*]pyridin-4-amine (54f). A mixture of **52** (300 mg, 890 μmol), 4-amino-1-benzyl piperidine (203 mg, 1.07 mmol), and diisopropylethylamine (229 μL, 1.34 mmol) in 2-propanol (5 mL) was heated in a microwave reactor at 120 °C for 12 min. The mixture was diluted with DCM and then purified by column chromatography on silica gel (gradient: 0 to 100% ethyl acetate in cyclohexane) to afford 449 mg (100%) of **54f** as a yellow residue. LCMS (Method 2, ESI): RT = 3.35 min, m+H = 492.6. ¹H NMR (400 MHz, CDCl₃) δ: 9.10 (s, 1 H), 8.18 (m, 2 H), 7.60 (m, 2 H), 7.51 (m, 2 H), 7.33 (m, 5 H), 6.69 (d, *J* = 4.2 Hz, 1 H), 4.00 (m, 1 H), 3.58 (m, 2 H), 2.85 (m, 2 H), 2.31 (m, 2 H), 2.11 (m, 2 H), 1.79 (m, 2 H).

1-[(1-Phenylmethyl)-piperidin-4-yl]-1,6-dihydro-imidazo[4,5-*d*]pyrrolo[2,3-*b*]pyridine (12). *Step 1:* *N*⁴-[1-(Phenylmethyl)-piperidin-3-yl]-1-phenylsulfonyl-1*H*-pyrrolo[2,3-*b*]pyridine-4,5-diamine. A mixture of **54f** (442 mg, 890 μmol), iron powder (201 mg, 3.60 mmol), and ammonium chloride (289 mg, 5.39 mmol) in methanol/water (12 mL, 3:1) was heated at reflux for 4 h. After cooling, the mixture was filtered through Celite, thoroughly washing the filter cake with methanol. The filtrate and washings were combined and concentrated under vacuum. The resulting residue was partitioned between DCM and water, the organic layer dried with sodium sulfate and concentrated under vacuum. Purification by column chromatography on silica gel (gradient: 0 to 10% methanol in DCM) afforded 321 mg (77%) of *N*⁴-[1-(phenylmethyl)-piperidin-3-yl]-1-phenylsulfonyl-1*H*-pyrrolo[2,3-*b*]pyridine-4,5-diamine as an off-white foam. LCMS (Method 2, ESI): RT = 2.55–2.68 min, m+H = 462.5. ¹H NMR (400 MHz, CDCl₃) δ: 8.12 (m, 2 H), 7.83 (s, 1 H), 7.52 (m, 1 H), 7.44 (m, 3 H), 7.34 (m, 5 H), 6.51 (d, *J* = 4.2 Hz, 1 H), 4.75 (m, 1 H), 3.69 (m, 3 H), 2.88 (m, 4 H), 2.29 (m, 2 H), 2.06 (m, 2 H), 1.71 (m, 2 H).

Step 2: 1-[(1-Phenylmethyl)-piperidin-4-yl]-6-(phenylsulfonyl)-1,6-dihydro-imidazo[4,5-*d*]pyrrolo[2,3-*b*]pyridine. A mixture of *N*⁴-[1-(phenylmethyl)-piperidin-3-yl]-1-phenylsulfonyl-1*H*-pyrrolo[2,3-*b*]pyridine-4,5-diamine (310 mg, 670 μmol), triethyl orthoformate (279 μL, 1.68 mmol), and *p*-toluenesulfonic acid mono-

hydrate (13 mg, 70 μmol) in toluene (10 mL) was heated to reflux for 2 h. After cooling, ethyl acetate was added and the mixture washed with saturated sodium hydrogen carbonate solution, water, and brine, dried with sodium sulfate, and concentrated under vacuum. Purification by column chromatography on silica gel (gradient: 0 to 10% MeOH in DCM) afforded 360 mg (100%) of 1-[1-(phenylmethyl)-piperidin-4-yl]-6-(phenylsulfonyl)-1,6-dihydro-imidazo[4,5-*d*]pyrrolo[2,3-*b*]pyridine as an orange/yellow residue. LCMS (Method 2, ESI): RT = 3.05 min, m+H = 472.5; ¹H NMR (400 MHz, CDCl₃) δ: 8.91 (s, 1 H), 8.22 (m, 2 H), 8.01 (br s, 1 H), 7.81 (d, *J* = 4.0 Hz, 1 H), 7.55 (m, 1 H), 7.47 (m, 2 H), 7.37 (m, 5 H), 6.83 (m, 1 H), 4.43 (m, 1 H), 3.62 (m, 2 H), 3.14 (m, 2 H), 2.21 (m, 6 H).

Step 3: 1-[(1-Phenylmethyl)-piperidin-4-yl]-1,6-dihydro-imidazo[4,5-*d*]pyrrolo[2,3-*b*]pyridine (12). A solution of 1-[1-(phenylmethyl)-piperidin-4-yl]-6-(phenylsulfonyl)-1,6-dihydro-imidazo[4,5-*d*]pyrrolo[2,3-*b*]pyridine (355 mg, 750 μmol) in methanol (18 mL) was treated with 1 M sodium hydroxide solution (8 mL) and left to stand at ambient temperature for 18 h. The mixture was partially concentrated under vacuum, and the resulting suspension was extracted twice with ethyl acetate. The combined organic extracts were washed with brine, dried with sodium sulfate, and concentrated under vacuum. Purification by column chromatography on silica gel (gradient: 0–10% methanol in DCM) afforded 189 mg (76%) of **12** as an off-white solid. LCMS (Method 1, ESI): RT = 1.92 min, m+H = 332.2; ¹H NMR (400 MHz, DMSO-*d*₆) δ: 11.85 (br s, 1 H), 8.58 (s, 1 H), 8.31 (s, 1 H), 7.48 (t, *J* = 3.0 Hz, 1 H), 7.36 (m, 4 H), 7.27 (m, 1 H), 6.75 (dd, *J* = 3.1, 1.9 Hz, 1 H), 4.57 (m, 1 H), 3.59 (s, 2 H), 3.01 (d, *J* = 11.3 Hz, 2 H), 2.31 (m, 2 H), 2.14 (m, 4 H).

1-Piperidin-4-yl-1,6-dihydro-imidazo[4,5-*d*]pyrrolo[2,3-*b*]pyridine (13). A stirred mixture of **12** (2.68 g, 8.09 mmol), ammonium formate (5.09 g, 80.9 mmol), and palladium hydroxide (20 wt % on carbon, 565 mg, 0.809 mmol) in methanol (150 mL) was heated at reflux for 5 h. Additional ammonium formate (5.09 g, 80.9 mmol) was added and heating continued for 3 h. After cooling, the mixture was filtered through Celite and then concentrated *in vacuo*. Purification by column chromatography on silica gel (gradient: 0 to 15% [2 M ammonia in methanol] in DCM) and subsequent trituration (diethyl ether) afforded 1.02 g (52%) of **13** as a beige solid. LCMS (Method 1, ESI): RT = 0.69 min, m+H = 242.2; ¹H NMR (400 MHz, DMSO-*d*₆) δ: 11.84 (s, 1 H), 8.58 (s, 1 H), 8.27 (s, 1 H), 7.46 (t, *J* = 2.9 Hz, 1 H), 6.78 (dd, *J* = 3.5, 1.8 Hz, 1 H), 4.61 (m, 1 H), 3.12 (m, 2 H), 2.77 (m, 2 H), 2.09–1.92 (m, 4 H).

1-(1-Methanesulfonyl-piperidin-4-yl)-1,6-dihydro-imidazo[4,5-*d*]pyrrolo[2,3-*b*]pyridine (19). To a stirred mixture of **13** (50.0 mg, 0.21 mmol) in DCM (2 mL), methanesulfonyl chloride (17.0 μL, 0.22 mmol) and triethylamine (57.0 μL, 0.41 mmol) were added sequentially. The mixture was stirred at room temperature for 30 min and then concentrated *in vacuo*. The resulting residue was triturated (water and then diethyl ether) and air-dried to afford 37.0 mg (55%) of **19** as a beige solid. LCMS (Method 1, ESI): RT = 2.02 min, m+H = 320.1. ¹H NMR (400 MHz, DMSO-*d*₆) δ: 11.86 (s, 1 H), 8.59 (s, 1 H), 8.34 (s, 1 H), 7.49 (t, *J* = 2.9 Hz, 1 H), 6.83 (dd, *J* = 3.1, 1.8 Hz, 1 H), 4.78 (m, 1 H), 3.77 (m, 2 H), 3.16 (m, 2 H), 2.98 (s, 3 H), 2.28–2.12 (m, 4 H).

4-(Imidazo[4,5-*d*]pyrrolo[2,3-*b*]pyridin-1(6*H*)-yl)-1-piperidin-1-yl)-propanenitrile (22). A solution of **13** (50 mg, 207 μmol) and acrylonitrile (27 μL, 414 μmol) in ethanol (5 mL) was heated at reflux for 5 h. The mixture was concentrated under vacuum and purified by column chromatography on silica gel (gradient: 0 to 10% in methanol in DCM) to afford 53 mg (87%) of **22** as a white solid. LCMS (Method 1, ESI): RT = 0.75 + 0.87 min, m+H = 295.1. ¹H NMR (DMSO-*d*₆) δ: 11.84 (s, 1 H), 8.58 (s, 1 H), 8.32 (s, 1 H), 7.46 (t, *J* = 3.0 Hz, 1 H), 6.76 (dd, *J* = 3.4, 1.9 Hz, 1 H), 4.58 (m, 1 H), 3.09 (d, *J* = 11.4 Hz, 2 H), 2.72 (m, 4 H), 2.37 (td, *J* = 11.3, 3.3 Hz, 2 H), 2.14 (m, 4 H).

(*S*)-1-Isopropylpyrrolidin-2-yl-[4-(imidazo[4,5-*d*]pyrrolo[2,3-*b*]pyridin-1(6*H*)-yl)-piperidin-1-yl]-methanone (26). To a stirred mixture of (*S*)-1-isopropylpyrrolidine-2-carboxylic acid (31.2 mg, 0.198 mmol), HATU (76 mg, 0.198 mmol), and *N,N*-diisopropylethylamine (40 μL, 0.247 mmol) in DMF (2 mL) was added **13** (40 mg,

0.165 mmol), and the resulting mixture was stirred at ambient temperature for 1 h. The reaction mixture was concentrated and purified by column chromatography on silica gel (gradient: 0 to 10% [2 M ammonia in methanol] in DCM) to afford 55 mg (88%) of **26**. LCMS (Method 1, ESI): RT = 1.57 min, m+H = 381.16. ¹H NMR (400 MHz, DMSO-*d*₆) δ: 11.85 (s, 1 H), 8.57 (s, 1 H), 8.30 (s, 1 H), 7.40 (t, *J* = 2.9 Hz, 1 H), 6.73 (d, *J* = 3.3 Hz, 1 H), 4.84 (t, *J* = 4.1 Hz, 1 H), 4.61 (d, *J* = 13.6 Hz, 3 H), 2.50–2.45 (m, 4 H), 2.20 (d, *J* = 12.6 Hz, 3 H), 2.07 (d, *J* = 3.8 Hz, 1 H), 2.01 (d, *J* = 12.5 Hz, 3 H), 1.81 (m, 4 H), 1.79 (t, *J* = 3.6 Hz, 2 H), 1.02 (dd, *J* = 22.8, 6.42 Hz, 1 H).

4-Benzoyloxycarbonylamino-4-methyl-piperidine-1-carboxylic Acid tert-Butyl Ester (56). Compound **55** (1.0 g, 4.11 mmol), triethylamine (830 μL, 5.96 mmol), and diphenylphosphoryl azide (1.2 mL, 5.59 mmol) in toluene were stirred at room temperature for 1 h. Benzyl alcohol (2.15 mL, 20.55 mmol) was added, and the reaction stirred at 80 °C for 18 h. The reaction mixture was cooled and concentrated under vacuum. Purification by column chromatography on silica gel (gradient: 0 to 25% ethyl acetate in cyclohexane) afforded 1.79 g of **56** (contaminated with benzyl alcohol). The material was used in the next step without further purification. LCMS (Method 3, ESI): RT = 3.86 min, m+H = 349.0.

4-Amino-4-methyl-piperidine-1-carboxylic Acid tert-Butyl Ester (57). A solution of **56** (1.8 g, 5.2 mmol) in ethanol was purged with argon, palladium on carbon (10% Pd content, 550 mg, 0.52 mmol) added, and the reaction mixture stirred under an atmosphere of hydrogen for 18 h. The solids were removed by filtration through Celite washing with ethanol and the filtrate concentrated under vacuum. Purification by column chromatography on silica gel (gradient: 0 to 5% [2 M ammonia in methanol] in DCM) afforded 525 mg (47%) of **57** as a clear oil. LCMS (Method 3, ESI): RT = 0.31 min, m+H = 214.9; ¹H NMR (400 MHz, CDCl₃) δ: 3.40–3.42 (m, 4 H), 1.48–1.51 (m, 2 H), 1.46 (s, 9 H), 1.36–1.39 (m, 2 H), 1.14 (s, 3 H).

4-Methyl-4-(imidazo[4,5-d]pyrrolo[2,3-b]pyridin-1(6H)-yl)-piperidine-1-carboxylic Acid tert-Butyl Ester (58). *Step 1*: 4-(5-Nitro-1-phenylsulfonyl-1H-pyrrolo[2,3-b]pyridine-4-ylamino)-4-methyl-piperidine-1-carboxylic Acid tert-Butyl Ester. A mixture of **52** (750 mg, 2.23 mmol), **57** (525 mg, 2.45 mmol), and *N,N*-diisopropylethylamine (1.36 mL, 7.80 mmol) in 2-propanol was heated at 95 °C for 64 h. The reaction mixture was cooled and the precipitate recovered by filtration. The solid was purified by column chromatography on silica gel (gradient: 0 to 30% ethyl acetate in cyclohexane) to afford 0.91 g (79%) of 4-(5-nitro-1-phenylsulfonyl-1H-pyrrolo[2,3-b]pyridine-4-ylamino)-4-methyl-piperidine-1-carboxylic acid tert-butyl ester as a yellow foam. LCMS (Method 3, ESI): RT = 4.35 min, m+H = 516.2.

Step 2: 4-(5-Amino-1-phenylsulfonyl-1H-pyrrolo[2,3-b]pyridine-4-ylamino)-4-methyl-piperidine-1-carboxylic Acid tert-Butyl Ester. A mixture of 4-(5-nitro-1-phenylsulfonyl-1H-pyrrolo[2,3-b]pyridine-4-ylamino)-4-methyl-piperidine-1-carboxylic acid tert-butyl ester (910 mg, 1.76 mmol), iron powder (~325 mesh, 393 mg, 7.04 mmol) and ammonium chloride (565 mg, 10.56 mmol) in a methanol/water mixture (3:1, 48 mL) was heated at 85 °C for 4 h. The cooled mixture was filtered through Celite washing with methanol. The filtrate was concentrated under vacuum and the residue obtained partitioned between saturated sodium bicarbonate solution and DCM. The aqueous phase was extracted twice with DCM. The combined extracts were washed with brine, dried (sodium sulfate), and concentrated under vacuum to afford a pink residue. Purification by column chromatography on silica gel (gradient: 0 to 4% [2 M ammonia in methanol] in DCM) afforded 720 mg (84%) of 4-(5-amino-1-phenylsulfonyl-1H-pyrrolo[2,3-b]pyridine-4-ylamino)-4-methyl-piperidine-1-carboxylic acid tert-butyl ester as an off-white foam. LCMS (Method 2, ESI): RT = 3.21 min, m+H = 486.3.

Step 3: 4-[6-Phenylsulfonyl-4-(imidazo[4,5-d]pyrrolo[2,3-b]pyridin-1(6H)-yl)]-4-methyl-piperidine-1-carboxylic Acid tert-Butyl Ester. A mixture of 4-(5-amino-1-phenylsulfonyl-1H-pyrrolo[2,3-b]pyridine-4-ylamino)-4-methyl-piperidine-1-carboxylic acid tert-butyl ester (720 mg, 1.48 mmol), triethyl orthoformate (615 μL, 3.70 mmol), and *p*-toluenesulfonic acid monohydrate (28.0 mg, 148 μmol) in toluene (50 mL) was heated at reflux for 24 h. After cooling, ethyl acetate was added and the mixture washed with saturated sodium hydrogen carbonate solution, water and brine, dried with sodium sulfate,

and concentrated under vacuum. Purification by column chromatography on silica gel (gradient: 0 to 4% [2 M ammonia in methanol] in DCM) afforded 630 mg (86%) of 4-[(6-phenylsulfonyl-4-(imidazo[4,5-d]pyrrolo[2,3-b]pyridin-1(6H)-yl)]-4-methyl-piperidine-1-carboxylic acid tert-butyl ester as an off-white foam. LCMS (Method 2, ESI): RT = 3.54 min, m+H = 496.2.

Step 4: 4-Methyl-4-(imidazo[4,5-d]pyrrolo[2,3-b]pyridin-1(6H)-yl)-piperidine-1-carboxylic Acid tert-Butyl Ester (**58**). A mixture of 4-[(6-phenylsulfonyl-4-(imidazo[4,5-d]pyrrolo[2,3-b]pyridin-1(6H)-yl)]-4-methyl-piperidine-1-carboxylic acid tert-butyl ester (630 mg, 1.27 mmol) and 1 M aqueous sodium hydroxide (6.36 mL, 6.36 mmol) in methanol/THF was stirred at room temperature for 60 h. The reaction mixture was concentrated under vacuum and the residue obtained partitioned between saturated sodium bicarbonate solution and DCM. The aqueous phase was extracted twice with DCM. The combined extracts were washed with brine, dried (sodium sulfate), and concentrated under vacuum to afford 440 mg (98%) of **58** as an off-white foam. LCMS (Method 1, ESI): RT 3.10 min, m+H = 356.2. ¹H NMR (400 MHz, DMSO-*d*₆) δ: 11.92 (s, 1 H), 8.62 (s, 1 H), 8.34 (s, 1 H), 7.45 (t, *J* = 3.1 Hz, 1 H), 6.62 (dd, *J* = 3.5, 1.9 Hz, 1 H), 3.71 (m, 2 H), 3.35 (br s, 2 H), 2.52–2.55 (m, 1 H), 2.04 (d, *J* = 13.5 Hz, 3 H), 1.85 (s, 3 H), 1.45 (s, 9 H).

1-(4-Methyl-piperidin-4-yl)-1,6-dihydro-imidazo[4,5-d]pyrrolo[2,3-b]pyridine (28). A solution of **58** (420 mg, 1.18 mmol) and TFA (7 mL) in DCM (28 mL) was stirred at room temperature for 1 h. The reaction mixture was concentrated under vacuum and a portion purified by column chromatography on silica gel (gradient: 0 to 10% [2 M ammonia in methanol] in DCM) to afford 77 mg of **28** as a white solid. LCMS (Method 1, ESI): RT 1.21 min, m+H = 278.2. ¹H NMR (400 MHz, DMSO-*d*₆) δ: 11.86 (s, 1 H), 8.61 (s, 1 H), 8.31 (s, 1 H), 7.47 (dd, *J* = 3.4, 2.6 Hz, 1 H), 7.01 (dd, *J* = 3.5, 1.9 Hz, 1 H), 2.82–2.85 (m, 4 H), 2.55 (dd, *J* = 13.5, 6.9 Hz, 2 H), 2.37 (br s, 1 H), 1.93–1.97 (m, 2 H), 1.81 (s, 3 H).

1-(1-Methanesulfonyl-4-methyl-piperidin-4-yl)-1,6-dihydro-imidazo[4,5-d]pyrrolo[2,3-b]pyridine (30). A mixture of **28** (136 mg, 0.53 mmol), methanesulfonyl chloride (41.5 μL, 0.53 mmol), and triethylamine (88.5 μL, 0.64 mmol) in DCM was stirred at room temperature for 1.5 h. The reaction mixture was washed with saturated sodium hydrogen carbonate solution and brine, dried with sodium sulfate, and concentrated under vacuum. Purification by column chromatography on silica gel (gradient: 0 to 6% [2 M ammonia in methanol] in DCM) afforded 102 mg (58%) of **30** as a white solid. LCMS (Method 1, ESI): RT 2.19 min, m+H = 334.3. ¹H NMR (400 MHz, DMSO-*d*₆) δ: 11.93 (s, 1 H), 8.63 (s, 1 H), 8.34 (s, 1 H), 7.52 (t, *J* = 3.1 Hz, 1 H), 6.79 (dd, *J* = 3.5, 1.9 Hz, 1 H), 3.32 (m, 6 H, includes water solvent peak), 2.92 (s, 3 H), 2.73 (m, 2 H), 2.19 (m, 2 H), 1.85 (s, 3 H).

trans-[4-(5-Nitro-1-phenylsulfonyl-1H-pyrrolo[2,3-b]pyridine-4-ylamino)-cyclohexyl]-carbamic Acid tert-Butyl Ester (60). A mixture of **52** (1.01 g, 3.0 mmol), **59** (707 mg, 3.30 mmol), and *N,N*-diisopropylethylamine (1.80 mL, 10.5 mmol) in 2-propanol was heated at 95 °C for 1 h. The cooled reaction mixture was concentrated under vacuum to afford a yellow residue. Purification by column chromatography on silica gel (gradient: 0 to 10% ethyl acetate in DCM) afforded 1.24 g (80%) of **60** as a yellow foam. LCMS (Method 3, ESI): RT = 4.13 min, m+H = 516.3.

trans-[4-(6-Phenylsulfonyl-4-(imidazo[4,5-d]pyrrolo[2,3-b]pyridin-1(6H)-yl)-cyclohexyl]-carbamic Acid tert-Butyl Ester (61). *Step 1*: *trans*-[4-(5-Amino-1-phenylsulfonyl-1H-pyrrolo[2,3-b]pyridine-4-ylamino)-cyclohexyl]-carbamic Acid tert-Butyl Ester. A mixture of **60** (1.14 g, 2.21 mmol), iron powder (~325 mesh, 494 mg, 8.84 mmol), and ammonium chloride (709 mg, 13.26 mmol) in a methanol/water mixture (3:1, 44 mL) was heated at reflux for 4 h. The cooled mixture was filtered through Celite washing with methanol. The filtrate was concentrated under vacuum and the residue obtained partitioned between saturated sodium bicarbonate solution and DCM. The aqueous phase was extracted twice with DCM. The combined extracts were washed with brine, dried (sodium sulfate), and concentrated under vacuum. Purification by column chromatography on silica gel (gradient: 0 to 5% methanol in DCM) afforded 940 mg (88%) of

trans-[4-(5-amino-1-phenylsulfonyl-1*H*-pyrrolo[2,3-*b*]pyridine-4-ylamino)-cyclohexyl]-carbamic acid *tert*-butyl ester as an off-white solid. LCMS (Method 3, ESI): RT = 2.65 min, m+H = 486.4.

Step 2: *trans*-[4-(6-phenylsulfonyl-4-(imidazo[4,5-*d*]pyrrolo[2,3-*b*]pyridin-1(6*H*)-yl)-cyclohexyl]-carbamic Acid *tert*-Butyl Ester (**61**). A mixture of *trans*-[4-(5-amino-1-phenylsulfonyl-1*H*-pyrrolo[2,3-*b*]pyridine-4-ylamino)-cyclohexyl]-carbamic acid *tert*-butyl ester (940 mg, 1.94 mmol), triethyl orthoformate (807 μ L, 4.85 mmol), and *p*-toluenesulfonic acid monohydrate (37.0 mg, 194 μ mol) in toluene (25 mL) was heated at reflux for 3.5 h. After cooling, ethyl acetate was added and the mixture washed with saturated sodium hydrogen carbonate solution, water, and brine, dried with sodium sulfate, and concentrated under vacuum. Purification by column chromatography on silica gel (gradient: 0 to 5% [2 M ammonia in methanol] in DCM) afforded 0.81 g (84%) of **61**. LCMS (Method 3, ESI): RT = 3.47 min, m+H = 496.2. ¹H NMR (400 MHz, CDCl₃) δ : 8.95 (s, 1 H), 8.23 (dd, *J* = 7.8, 1.3 Hz, 3 H), 7.85 (d, *J* = 4.0 Hz, 1 H), 7.55 (m, 1 H), 7.47–7.48 (m, 2 H), 6.75 (d, *J* = 4.0 Hz, 1 H), 4.40–4.47 (m, 2 H), 3.63 (br s, 1 H), 2.33 (m, 5 H), 1.99 (m, 2 H), 1.47 (s, 9 H).

trans-[4-(Imidazo[4,5-*d*]pyrrolo[2,3-*b*]pyridin-1(6*H*)-yl)-cyclohexyl]-carbamic Acid *tert*-Butyl Ester (**33**). A mixture of **61** (810 mg, 1.63 mmol) and 1 M aqueous sodium hydroxide (8.2 mL, 8.2 mmol) in methanol/THF was stirred at room temperature for 18 h. The reaction mixture was concentrated under vacuum and the residue partitioned between saturated sodium bicarbonate solution and DCM. The aqueous phase was extracted twice with DCM. The combined extracts were washed with brine, dried (sodium sulfate), and concentrated under vacuum. Purification by column chromatography on silica gel (gradient: 0 to 6% [2 M ammonia in methanol] in DCM) afforded 470 mg (81%) of **33** as a white solid. LCMS (Method 1, ESI): RT 3.06 min, m+H = 356.2. ¹H NMR (400 MHz, DMSO-*d*₆) δ : 11.84 (s, 1 H), 8.57 (s, 1 H), 8.28 (s, 1 H), 7.47 (t, *J* = 3.0 Hz, 1 H), 6.89 (d, *J* = 7.6 Hz, 1 H), 6.68 (dd, *J* = 3.4, 1.9 Hz, 1 H), 4.51–4.54 (m, 1 H), 3.43 (br s, 1 H), 2.16 (d, *J* = 11.7 Hz, 2 H), 2.00 (d, *J* = 12.4 Hz, 4 H), 1.51–1.56 (m, 2 H), 1.41 (s, 9 H).

trans-4-(Imidazo[4,5-*d*]pyrrolo[2,3-*b*]pyridin-1(6*H*)-yl)-cyclohexylamine (**35**). A mixture of **33** (442 mg, 1.24 mmol) and TFA (4 mL) in DCM (16 mL) was stirred at room temperature for 1.5 h. The reaction mixture was concentrated under vacuum and the residue purified by chromatography on an SCX-2 column (gradient: 10 to 50% [2 M ammonia in methanol] in DCM) to afford 300 mg (95%) of **35** as a white solid. LCMS (Method 1, ESI): RT 0.75 min, m+H = 256.1. ¹H NMR (400 MHz, DMSO-*d*₆) δ : 11.84 (br s, 1 H), 8.57 (s, 1 H), 8.26 (s, 1 H), 7.47 (d, *J* = 3.4 Hz, 1 H), 6.71 (d, *J* = 3.4 Hz, 1 H), 4.51–4.54 (m, 1 H), 2.73–2.75 (m, 1 H), 2.13 (d, *J* = 11.7 Hz, 2 H), 1.94–1.98 (m, 4 H), 1.40–1.43 (m, 2 H).

trans-3-[4-(Imidazo[4,5-*d*]pyrrolo[2,3-*b*]pyridin-1(6*H*)-yl)-cyclohexylamino]-propionitrile (**41**). A mixture of acrylonitrile (64.5 μ L, 0.98 mmol) and **35** (50.0 mg, 196 μ mol) in ethanol (5.5 mL) was heated at 80 °C for 1 h. After cooling, the solvent was removed under vacuum. The resulting residue was triturated (water and then diethyl ether) and air-dried to afford 22.0 mg (36%) of **41** as a cream colored solid. LCMS (Method 1, ESI): RT = 1.22 min, m+H = 309.2. ¹H NMR (400 MHz, DMSO-*d*₆) δ : 11.83 (s, 1 H), 8.57 (s, 1 H), 8.26 (s, 1 H), 7.46 (t, *J* = 2.6 Hz, 1 H), 6.73 (dd, *J* = 3.1, 1.8 Hz, 1 H), 4.57 (m, 1 H), 2.83 (t, *J* = 6.6 Hz, 2 H), 2.59 (m, 3 H), 2.17 (m, 2 H), 2.06 (m, 2 H), 1.95 (m, 3 H), 1.40 (m, 2 H).

(±)-cis-(3-Hydroxy-cyclopentyl)-carbamic Acid *tert*-Butyl Ester (**68**). A solution of **67**⁴³ in ethanol (90 mL) was treated with 10% palladium on carbon (1.0 g, 0.94 mmol palladium) and hydrogenated for 3 days at ambient pressure. More catalyst was added (1.2 g, 1.1 mmol palladium), and the mixture was hydrogenated for a further 24 h. The suspension was filtered through Celite washing with ethanol. The filtrate was concentrated under vacuum to afford 8.86 g (97%) of **68** as a dark green oil. LCMS (Method 2, ESI): RT = 3.08 min, m+H = 200. ¹H NMR (400 MHz, CDCl₃) δ : 4.71 (m, 1 H), 4.54 (m, 1 H), 1.87 (m, 3 H), 1.68 (m, 3 H), 1.50 (s, 9 H).

(±)-trans-(3-Hydroxy-cyclopentyl)-carbamic Acid *tert*-Butyl Ester (**69**). **Step 1:** A solution of **68** (3.00 g, 14.9 mmol) in dry THF (81 mL) at 0 °C under an inert atmosphere was treated with triphenylphosphine (4.30 g, 16.4 mmol) and diisopropylazodicarboxylate

(3.50 mL, 17.9 mmol) and the mixture stirred at 0 °C for 10 min. A solution of acetic acid (2.4 mL, 41.8 mmol) in dry THF (18 mL) was added dropwise and the mixture stirred at 0 °C for 20 min, then at ambient temperature overnight. The mixture was concentrated under vacuum and the residue obtained purified by column chromatography on silica gel (gradient: 0 to 30% EtOAc in cyclohexane) to afford 2.87 g (79%) of **(±)-trans**-acetic acid 3-*tert*-butoxycarbonylamino-cyclopentyl ester as a white solid. LCMS (Method 2, ESI): RT = 3.23 min, no m+H observed. ¹H NMR (400 MHz, CDCl₃) δ : 5.18 (m, 1 H), 4.46 (br s, 1 H), 4.14 (m, 1 H), 2.12 (m, 3 H), 2.01 (s, 3 H), 1.69 (m, 2 H), 1.44 (s, 9 H), 1.41 (m, 1 H). **Step 2:** A solution of the preceding material (2.27 g, 11.8 mmol) in methanol (6.8 mL) and THF (6.8 mL) was treated with 4 M aqueous sodium hydroxide solution (6.8 mL, 27.2 mmol) and the mixture stirred at ambient temperature for 1.5 h. The mixture was concentrated under vacuum and the residue obtained partitioned between DCM and brine. The aqueous phase was extracted twice with DCM, and the combined extracts were washed with brine, dried (sodium sulfate), and concentrated under vacuum to afford 2.28 g (96%) of **69** as a white solid. LCMS (Method 2, ESI): RT = 2.46 min, m+H = 202 (weak), m+H+MeCN = 243. ¹H NMR (400 MHz, CDCl₃) δ : 4.45 (br s, 1 H), 4.40 (m, 1 H), 4.17 (m, 1 H), 2.21 (m, 1 H), 2.02 (m, 2 H), 1.62 (m, 2 H), 1.44 (s, 9 H), 1.40 (m, 1 H).

(±)-trans-(3-Amino-cyclopentyl)-carbamic Acid *tert*-Butyl Ester (**70**). **Step 1:** A solution of **68** (2.10 g, 10.4 mmol) in acetone (44 mL) containing triethylamine (2.91 mL, 20.9 mmol) was cooled to 0 °C and treated dropwise with methanesulfonyl chloride (1.21 mL, 15.7 mmol). After 10 min, the mixture was concentrated under vacuum and the residue obtained partitioned between EtOAc and water. The aqueous phase was extracted twice with ethyl acetate, and the combined extracts were washed with 10% aqueous citric acid solution, saturated sodium hydrogen carbonate solution, and brine, dried (sodium sulfate), and concentrated under vacuum to afford 2.88 g (99%) of **(±)-cis**-methanesulfonic acid 3-*tert*-butoxycarbonylamino-cyclopentyl ester as a cream colored solid. LCMS (Method 2, ESI): RT = 2.97 min, m+H = 280 (weak), m+H+MeCN = 343. ¹H NMR (400 MHz, CDCl₃) δ : 5.14 (m, 1 H), 4.72 (br s, 1 H), 4.12 (br s, 1 H), 3.01 (s, 3 H), 2.36 (m, 1 H), 2.11 (m, 2 H), 1.94 (m, 1 H), 1.87 (m, 1 H), 1.70 (m, 1 H), 1.44 (s, 9 H). **Step 2:** A solution of **(±)-cis**-methanesulfonic acid 3-*tert*-butoxycarbonylamino-cyclopentyl ester (2.88 g, 10.3 mmol) in DMF (21 mL) was treated with a solution of sodium azide (0.94 g, 14.5 mmol) in water (3.7 mL), and the reaction mixture was heated at 100 °C for 1 h. The cooled mixture was concentrated under vacuum and the residue obtained partitioned between ethyl acetate and water. The aqueous phase was extracted twice with ethyl acetate, and the combined extracts were washed with water and brine, dried (sodium sulfate), and concentrated under vacuum to afford 2.24 g (96%) of **(±)-trans**-(3-azido-cyclopentyl)-carbamic acid *tert*-butyl ester as a yellow oil. LCMS (Method 2, ESI): RT = 3.48 min, no m+H observed, m+H+MeCN = 290. ¹H NMR (400 MHz, CDCl₃) δ : 4.45 (br s, 1 H), 4.09 (br s, 1 H), 4.03 (m, 1 H), 2.10 (m, 3 H), 1.71 (m, 2 H), 1.44 (m, 10 H). **Step 3:** A solution of **(±)-trans**-(3-azido-cyclopentyl)-carbamic acid *tert*-butyl ester (2.24 g, 9.9 mmol) in THF (90 mL) was treated with water (9 mL) then triphenylphosphine (2.86 g, 10.9 mmol), and the reaction mixture was heated to 55 °C overnight. The cooled mixture was concentrated under vacuum to a solid residue. The solid was triturated with ether and filtered, rinsing with ether. The filtrate was concentrated under vacuum to a yellow oil then triturated with ether as before. The filtrate was concentrated to an orange oil that was purified by column chromatography on silica gel (gradient: 0 to 15% methanol in DCM plus 1% triethylamine) to afford 1.80 g (91%) of **70** as a white paste that crystallized on standing. LCMS (Method 2, ESI): RT = 0.84 min, m+H = 201. ¹H NMR (400 MHz, CDCl₃) δ : 4.47 (br s, 1 H), 4.10 (br s, 1 H), 3.46 (m, 1 H), 2.18 (m, 1 H), 2.00 (m, 1 H), 1.72 (t, *J* = 6.7 Hz, 2 H), 1.44 (s, 9 H), 1.34 (m, 4 H).

(±)-trans-[3-(6-Phenylsulfonyl-imidazo[4,5-*d*]pyrrolo[2,3-*b*]pyridin-1(6*H*)-yl)-cyclopentyl]-carbamic Acid *tert*-Butyl Ester (**72**). **Step 1:** A solution of **70** (1.70 g, 8.5 mmol) in 2-propanol (21 mL) was treated with *N,N*-diisopropylethylamine (1.60 mL, 9.2 mmol)

followed by **52** (2.39 g, 7.1 mmol), and the mixture was heated at 120 °C for 10 min using microwave irradiation. The cooled reaction mixture was filtered, and the solid was rinsed with 2-propanol and dried under vacuum to afford 3.00 g (84%) of (\pm)-*trans*-[3-(5-nitro-1-phenylsulfonyl-1*H*-pyrrolo[2,3-*b*]pyridin-4-ylamino)-cyclopentyl]-carbamic acid *tert*-butyl ester as a yellow crystalline solid. LCMS (Method 2, ESI): RT = 4.09 min, m+H = 502. ¹H NMR (400 MHz, CDCl₃) δ : 9.09 (s, 1 H), 9.06 (d, *J* = 7.0 Hz, 1 H), 8.19 (d, *J* = 8.0 Hz, 2 H), 7.62 (m, 2 H), 7.52 (t, *J* = 8.0 Hz, 2 H), 6.84 (d, *J* = 4.2 Hz, 1 H), 4.58 (m, 2 H), 4.11 (m, 1 H), 2.36 (m, 1 H), 2.25 (m, 1 H), 2.10 (m, 2 H), 1.73 (m, 1 H), 1.62 (m, 1 H), 1.45 (s, 9 H). *Step 2*: A suspension of (\pm)-*trans*-[3-(5-nitro-1-phenylsulfonyl-1*H*-pyrrolo[2,3-*b*]pyridin-4-ylamino)-cyclopentyl]-carbamic acid *tert*-butyl ester (3.0 g, 6.0 mmol) in ethanol (22 mL) was treated with water (8 mL), ammonium chloride (1.92 g, 35.9 mmol), and iron powder (1.34 g, 24.0 mmol) and the mixture heated at 80 °C for 1.5 h. The cooled reaction mixture was filtered through Celite washing with ethanol/water. The filtrate was concentrated under vacuum and the residue obtained partitioned between DCM and a saturated sodium hydrogen carbonate solution. The aqueous phase was extracted twice with DCM, and the combined extracts were washed with brine, dried (sodium sulfate), and concentrated under vacuum to afford a beige foam. The foam was crystallized from DCM to afford 1.45 g (51%) of (\pm)-*cis*-[3-(5-amino-1-phenylsulfonyl-1*H*-pyrrolo[2,3-*b*]pyridin-4-ylamino)-cyclopentyl]-carbamic acid *tert*-butyl ester as a white solid. LCMS (Method 2, ESI): RT = 2.85 min, m+H = 472. ¹H NMR (400 MHz, CDCl₃) δ : 8.13 (d, *J* = 8.1 Hz, 2 H), 7.85 (s, 1 H), 7.54 (tt, *J* = 7.5, 1.3 Hz, 1 H), 7.45 (m, 3 H), 6.62 (d, *J* = 4.4 Hz, 1 H), 4.99 (br s, 1 H), 4.56 (br s, 1 H), 4.41 (br s, 1 H), 4.16 (br s, 1 H), 2.24 (m, 2 H), 2.07 (br s, 1 H), 1.88 (m, 1 H), 1.63 (m, 1 H), 1.50 (m, 1 H), 1.44 (s, 9 H). The mother liquor was concentrated under vacuum to a brown foam that was crystallized from DCM to provide a second crop (0.34 g, 12%). The mother liquors from the second crop were concentrated under vacuum to a brown foam. Purification by column chromatography on silica gel (gradient: 0 to 7% methanol in DCM) afforded a further crop of 0.46 g (16%) of product as a white solid. *Step 3*: A suspension of (\pm)-*cis*-[3-(5-amino-1-phenylsulfonyl-1*H*-pyrrolo[2,3-*b*]pyridin-4-ylamino)-cyclopentyl]-carbamic acid *tert*-butyl ester (1.25 g, 2.7 mmol) in toluene (12.5 mL) was treated with triethyl orthoformate (1.3 mL, 8.0 mmol) followed by *p*-toluene sulfonic acid monohydrate (50 mg, 0.27 mmol), and the reaction mixture was heated to 100 °C for 1.75 h. The cooled reaction mixture was filtered, and the filter cake was washed with toluene and water and dried to afford a white solid. Purification by column chromatography on silica gel (gradient: 0 to 7% methanol in DCM) afforded 0.90 g (70%) of **72** as a white solid. LCMS (Method 2, ESI): RT = 3.59 min, m+H = 482. ¹H NMR (400 MHz, DMSO-*d*₆) δ : 8.72 (s, 1 H), 8.49 (s, 1 H), 8.13 (d, *J* = 8.5 Hz, 2 H), 8.01 (d, *J* = 4.2 Hz, 1 H), 7.70 (tt, *J* = 7.7, 1.2 Hz, 1 H), 7.61 (t, *J* = 8.1 Hz, 2 H), 7.29 (d, *J* = 4.0 Hz, 1 H), 7.18 (d, *J* = 4.7 Hz, 1 H), 5.23 (p, *J* = 7.7 Hz, 1 H), 4.11 (m, 1 H), 2.36 (m, 1 H), 2.29 - 2.08 (m, 3 H), 1.96 (m, 1 H), 1.64 (m, 1 H), 1.40 (s, 9 H).

(\pm)-*trans*-3-(Imidazo[4,5-*d*]pyrrolo[2,3-*b*]pyridin-1(6*H*)-yl)-cyclopentyl]-carbamic Acid *tert*-Butyl Ester (**47**). A suspension of **72** (300 mg, 0.62 mmol) in methanol (3.2 mL) and THF (3.2 mL) was treated with 2 M aqueous sodium hydroxide solution (1.6 mL, 3.2 mmol), and the mixture was stirred at ambient temperature for 30 min then at 50 °C for 1 h. The mixture was concentrated under vacuum and the residue obtained partitioned between DCM and water. The aqueous phase was extracted with DCM, and the combined extracts were washed with saturated sodium hydrogen carbonate solution, and brine, dried (sodium sulfate), and concentrated under vacuum to afford a yellow glass. This was triturated with ether to give a solid that was collected, washed with ether, and dried to afford 170 mg (80%) of **47** as an off-white solid. LCMS (Method 1, ESI): RT = 2.93 min, m+H = 342.3; ¹H NMR (400 MHz, DMSO-*d*₆) δ : 11.83 (s, 1 H), 8.57 (s, 1 H), 8.29 (s, 1 H), 7.47 (t, *J* = 3.0 Hz, 1 H), 7.20 (d, *J* = 7.3 Hz, 1 H), 6.83 (dd, *J* = 3.2, 1.7 Hz, 1 H), 5.24 (q, *J* = 7.5 Hz, 1 H), 4.13 (m, 1 H), 2.38 (m, 1 H), 2.33 - 2.12 (m, 3 H), 2.03 (m, 1 H), 1.68 (m, 1 H), 1.40 (s, 9 H).

trans-3-(Imidazo[4,5-*d*]pyrrolo[2,3-*b*]pyridin-1(6*H*)-yl)-cyclopentyl]-carbamic Acid *tert*-Butyl Ester (**49**). Compound **47** was resolved using SFC (21.2 × 250 mm, 5 μ m Chiralpak AD; mobile phase, 35% methanol/65% CO₂; flow rate, 60 mL/min; detection at 230 nm). LCMS (Method 4, ESI): RT = 0.94 min, m = 341.2.

■ ASSOCIATED CONTENT

Supporting Information

Details of crystallographic methods and procedures; analytical LCMS methods; experimental LogD measurement procedures; *in vitro* and *in vivo* ADME experimental procedures; details of molecular modeling calculations and methods; preparation and characterization of **7–11**, **14–18**, **20**, **21**, **23–25**, **27**, **29**, **31**, **32**, **34**, **36–40**, **42–46**, **48**, **54b–d**, **54g**, **62**, **64–66**, **71**, **73**, and **74**. This material is available free of charge via the Internet at <http://pubs.acs.org>.

Accession Codes

PDB nos.: 4E6D for **7** complexed with JAK2TM, 4E6Q for **12** complexed with JAK2TM, 4ESW for **26** complexed with JAK1, 4E4L for **30** complexed with JAK1, 4E4M for **30** complexed with JAK2, and 4E4N for **49** complexed with JAK1.

■ AUTHOR INFORMATION

Corresponding Author

*Tel: +44 1279 645624. Fax: +44 1279 645646. E-mail: janusz.kulagowski@glpg.

Present Addresses

▽ Department of Infectious Disease, MedImmune, Gaithersburg, Maryland, United States.

◆ Cancer Research UK Drug Discovery Unit, Paterson Institute for Cancer Research, University of Manchester, Wilmslow Road, Manchester M20 4BX, United Kingdom.

Notes

The authors declare no competing financial interest.

■ ACKNOWLEDGMENTS

We wish to thank Peter Crackett for the provision of intermediates, Russell Scammel, Michael Podmore and Neil Bayliss for analytical support, Erle Delarosa (hepatocyte stability), and Ning Liu (microsomal stability) for *in vitro* ADME support, and Peter Dragovich and David Clark for editorial assistance.

■ ABBREVIATIONS USED

AcOH, Acetic acid; BME, β -mercaptoethanol; CDCl₃, deuterated chloroform; DMSO-*d*₆, deuterated DMSO; EDCl, 1-ethyl-3-(3-dimethylaminopropyl) carbodiimide hydrochloride; HATU, 2-(7-aza-1*H*-benzotriazole-1-yl)-1,1,3,3-tetramethyluronium hexafluorophosphate; HOBt, hydroxybenzotriazole; LogD_{7.2}, log of partition coefficient between octanol and pH_{7.2} aqueous buffer; MCT, methyl cellulose/tween; MDCK, Madin–Darby canine kidney cells; *P*_{app}, apparent permeability; *p*-TsOH, *para*-toluenesulfonic acid; SCX-2, prepacked Isolute silica-based sorbent with a chemically bonded propylsulfonic acid functional group; TCEP, *tris*(2-carboxyethyl)phosphine

■ REFERENCES

- (1) (a) Song, L.; Schindler, C. JAK-STAT Signalling. In *The Handbook of Cell Signalling*. 2nd ed.; Bradshaw, R. A., Dennis, E. A., Eds.; Elsevier Inc.: San Diego, CA, 2010; Vol. 3, pp 2041–2048. (b) Shuai, K.; Liu, B. Regulation of JAK-STAT Signalling in the Immune System. *Nat. Rev. Immunol.* **2003**, *3*, 900–911. (c) Ghoreschi, K.; Laurence, A.; O’Shea, J. J. Janus Kinases in Immune Cell Signalling. *Immunol. Rev.* **2009**, *228*, 273–287.

- (2) (a) Levy, D. E.; Darnell, J. E., Jr. STATS: Transcriptional Control and Biological Impact. *Nat. Rev. Mol. Cell Biol.* **2002**, *3*, 651–662. (b) Kisseleva, T.; Bhattacharya, S.; Braunstein, J.; Schindler, C. W. Signalling Through the JAK/STAT Pathway, Recent Advances and Future Challenges. *Gene* **2002**, *285*, 1–24.
- (3) Schindler, C.; Levy, D. E.; Decker, T. JAK-STAT Signaling: From Interferons to Cytokines. *J. Biol. Chem.* **2007**, *282*, 20059–20063.
- (4) Quintas-Cardama, A.; Kantarjian, H.; Cortes, J.; Verstovsek, S. Janus Kinase Inhibitors for the Treatment of Myeloproliferative Neoplasias and Beyond. *Nat. Rev. Drug Discovery* **2011**, *10*, 127–140.
- (5) Watford, W. T.; O'Shea, J. J. Human TYK2 Kinase Deficiency: Another Primary Immunodeficiency Syndrome. *Immunity* **2006**, *25*, 695–697.
- (6) O'Shea, J. J.; Gadina, M.; Schreiber, R. D. Cytokine Signaling in 2002: New Surprises in the Jak/Stat Pathway. *Cell* **2002**, *109* (Suppl.), S121–S131.
- (7) O'Shea, J. J.; Pesu, M.; Borie, D. C.; Changelian, P. S. A New Modality for Immunosuppression: Targeting the JAK/STAT Pathway. *Nat. Rev. Drug Discovery* **2004**, *3*, 555–564.
- (8) (a) Wroblewski, S. T.; Pitts, W. J. Advances in the Discovery of Small Molecule JAK3 Inhibitors. In *Annual Reports in Medicinal Chemistry*; Macor, J. E., Ed.; Elsevier Inc.: San Diego, 2009; Vol. 44, Chapter 12, pp 247–264. (b) Changelian, P. S.; Flanagan, M. E.; Ball, D. J.; Kent, C. R.; Magnuson, K. S.; Martin, W. H.; Rizzuti, B. J.; Sawyer, P. S.; Perry, B. D.; Brissette, W. H.; McCurdy, S. P.; Kudlacz, E. M.; Conklyn, M. J.; Elliott, E. A.; Koslov, E. R.; Fisher, M. B.; Strelevitz, T. J.; Yoon, K.; Whipple, D. A.; Sun, J.; Munchhof, M. J.; Doty, J. L.; Casavant, J. M.; Blumenkopf, T. A.; Hines, M.; Brown, M. F.; Lillie, B. M.; Subramanyam, C.; Shang-Poa, C.; Milici, A. J.; Beckius, G. E.; Moyer, J. D.; Su, C.; Woodworth, T. G.; Gaweco, A. S.; Beals, C. R.; Littman, B. H.; Fisher, D. A.; Smith, J. F.; Zagouras, P.; Magna, H. A.; Saltarelli, M. J.; Johnson, K. S.; Nelms, L. F.; Des Etages, S. G.; Hayes, L. S.; Kawabata, T. T.; Finco-Kent, D.; Baker, D. L.; Larson, M.; Si, M. S.; Paniagua, R.; Higgins, J.; Holm, B.; Reitz, B.; Zhou, Y. J.; Morris, R. E.; O'Shea, J. J.; Borie, D. C. Prevention of Organ Allograft Rejection by a Specific Janus Kinase 3 Inhibitor. *Science* **2003**, *302*, 875–878.
- (9) (a) West, K. CP-690550, a JAK3 Inhibitor as an Immunosuppressant for the Treatment of Rheumatoid Arthritis, Transplant Rejection, Psoriasis and Other Immune-mediated Disorders. *Expert Opin. Invest. Drugs* **2009**, *10*, 491–504. (b) Verstovsek, S. Janus-Activated Kinase 2 Inhibitors: A New Era of Targeted Therapies Providing Significant Clinical Benefit for Philadelphia Chromosome-Negative Myeloproliferative Neoplasms. *J. Clin. Oncology* **2011**, *29*, 781–788. (c) Vijayakrishnan, L.; Venkataramanan, R.; Gulati, P. Treating Inflammation with the Janus Kinase Inhibitor CP-690,550. *Trends Pharmacol. Sci.* **2011**, *32*, 25–34.
- (10) Meyer, D. M.; Jesson, M. I.; Li, X.; Elrick, M. M.; Funckes-Shippy, C. L.; Warner, J. D.; Gross, C. J.; Dowty, M. E.; Ramaiah, S. K.; Hirsch, J. L.; Sabbye, M. J.; Barks, J. L.; Kishore, N.; Morris, D. L. Anti-Inflammatory Activity and Neutrophil Reductions Mediated by the JAK1/JAK3 Inhibitor, CP-690,550, in Rat Adjuvant-Induced Arthritis. *J. Inflamm.* **2010**, *7*, 41.
- (11) (a) Lucia, E.; Recchia, A. G.; Gentile, M.; Bossio, S.; Vigna, E.; Mazzone, C.; Madeo, A.; Morabito, L.; Gigliotti, V.; DeStefano, L.; Caruso, N.; Servillo, P.; Franzese, F.; Bisconte, M. G.; Gentile, C.; Morabito, F. Janus Kinase 2 Inhibitors in Myeloproliferative Disorders. *Expert Opin. Invest. Drugs* **2011**, *20*, 41–59. (b) Ghoreschi, K.; Laurence, A.; O'Shea, J. J. Selectivity and Therapeutic Inhibition of Kinases: To Be or Not To Be? *Nat. Immunol.* **2009**, *4*, 356–360.
- (12) Mesa, R. A.; Yasothan, U.; Kirkpatrick, P. Ruxolitinib. *Nat. Rev. Drug Discovery* **2012**, *11*, 103–104.
- (13) Moreland, L. A Randomized Placebo-Controlled Study of INCB018424, a Selective Janus Kinase 1&2 (JAK1&2) Inhibitor in Rheumatoid Arthritis (RA). Annual Scientific Meeting of the American College of Rheumatology, San Francisco, CA, Oct 24–29, 2008; John Wiley & Sons: Chichester, UK; Abstract 714.
- (14) Quintas-Cardama, A.; Vaddi, K.; Liu, P.; Manshour, T.; Li, J.; Scherle, P. A.; Caulder, E.; Wen, X.; Li, Y.; Waeltz, P.; Rupar, M.; Burn, T.; Lo, Y.; Kelley, J.; Covington, M.; Shepard, S.; Rodgers, J. D.; Haley, P.; Kantarjian, H.; Fridman, J. S.; Verstovsek, S. Preclinical Characterization of the Selective JAK1/2 Inhibitor INCB018424: Therapeutic Implications for the Treatment of Myeloproliferative Neoplasms. *Blood* **2010**, *115*, 3109–3117.
- (15) Haan, C.; Rolvering, C.; Raulf, F.; Kapp, M.; Druckes, P.; Thoma, G.; Behrmann, I.; Zerwes, H.-G. Jak1 Has a Dominant Role over Jak3 in Signal Transduction through γ c-Containing Cytokine Receptors. *Chem. Biol.* **2011**, *18*, 314–323.
- (16) Rodig, S. J.; Meraz, M. A.; White, J. M.; Lampe, P. A.; Riley, J. K.; Arthur, C. D.; King, K. L.; Sheehan, K. C. F.; Yin, L.; Pennica, D.; Johnson, E. M., Jr; Schreiber, R. D. Disruption of the JAK1 Gene Demonstrates Obligatory and Nonredundant Roles of the JAKs in Cytokine-Induced Biologic Responses. *Cell* **1998**, *93*, 373–383.
- (17) Parganas, E.; Wang, D.; Stravopodis, D.; Topham, D. J.; Marine, J.-C.; Teglund, S.; Vanin, E. F.; Bodner, S.; Colamonici, O. R.; van Deursen, J. M.; Grosveld, G.; Ihle, J. N. JAK2 Is Essential for Signaling Through a Variety of Cytokine Receptors. *Cell* **1998**, *93*, 385–395.
- (18) Shimoda, K.; Kato, K.; Aoki, K.; Matsuda, T.; Miyamoto, A.; Shibamori, M.; Yamashita, M.; Numata, A.; Takase, K.; Kobayashi, S.; Shibata, S.; Asano, Y.; Gondo, H.; Sekiguchi, K.; Nakayama, K.; Nakayama, T.; Okamura, T.; Okamura, S.; Niho, Y.; Nakayama, K. TYK2 Plays a Restricted Role in IFN α Signaling, Although it is Required for IL-12-Mediated T Cell Function. *Immunity* **2000**, *13*, 561–571.
- (19) Patel, A. M.; Moreland, L. W. Interleukin-6 Inhibition for Treatment of Rheumatoid Arthritis: A Review of Tocilizumab Therapy. *Drug Des. Dev. Ther.* **2010**, *4*, 263–278.
- (20) Baslund, B.; Tvede, N.; Danneskiold-Samsøe, B.; Larsson, P.; Panavi, G.; Petersen, J.; Petersen, L. J.; Beurskens, F. J.; Schuuman, J.; van de Winkel, J. G.; Parren, P. W.; Gracie, J. A.; Jongbloed, S.; Liew, F. Y.; McInnes, I. B. Targeting Interleukin-15 in Patients With Rheumatoid Arthritis: A Proof-of-Concept Study. *Arthritis Rheum.* **2005**, *52*, 2686–2692.
- (21) (a) Yamaoka, K.; Kubo, S.; Sonomoto, K.; Maeshima, K.; Tanaka, Y. JAK Inhibitor: Tofacitinib, a New Disease Modifying Anti-Rheumatic Drug. *Inflammation Regener.* **2011**, *31*, 349–353. (b) Fleischmann, R.; Cutolo, M.; Genovese, M. C.; Lee, E. B.; Kanik, K. S.; Sadi, S.; Connell, C. A.; Gruben, D.; Krishnaswami, S.; Wallenstein, G.; Wilkinson, B. E.; Zwillich, S. H. Phase 2B Dose-Ranging Study of the Oral JAK Inhibitor Tofacitinib (CP-690,550) or Adalimumab Monotherapy Versus Placebo in Patients with Active Rheumatoid Arthritis with an Inadequate Response to DMARDs. *Arthritis Rheum.* **2012**, *64*, 617–629. (c) Kremer, J. M.; Cohen, S.; Wilkinson, B. E.; Connell, C. A.; French, J. L.; Gomez-Reino, J.; Gruben, D.; Kanik, K. S.; Krishnaswami, S.; Pascuala-Ramos, V.; Wallenstein, G.; Zwillich, S. H. A Phase 2B Dose-Ranging Study of the Oral JAK Inhibitor Tofacitinib (CP-690,550) Versus Placebo in Combination with Background Methotrexate in Patients with Active Rheumatoid Arthritis and Inadequate Response to Methotrexate Alone. *Arthritis Rheum.* **2012**, *64*, 970–981.
- (22) (a) Jatiani, S. S.; Baker, S. J.; Silverman, L. R.; Reddy, E. P. JAK/STAT Pathways in Cytokine Signaling and Myeloproliferative Disorders: Approaches for Targeted Therapies. *Genes Cancer* **2010**, *1*, 979–993. (b) Verstovsek, S.; Passamonti, F.; Rambaldi, A.; Barosi, G.; Rosen, P.; Levy, R.; Bradley, E. C.; Schacter, L.; Garrett, W. M.; Vaddi, K.; Contel, N.; Rumi, E.; Gattoni, E.; Cazzola, M.; Kantarjian, H.; Barbui, T.; Vannucchi, A. A Phase 2 Study of INCB018424, an Oral, Selective JAK1/JAK2 Inhibitor, in Patients with Advanced Polycythemia Vera (PV) and Essential Thrombocythemia (ET) Refractory to Hydroxyurea; 51st American Society of Hematology Annual Meeting and Exposition, New Orleans, LA, Dec 5–8, 2009; American Society of Hematology: Washington, DC; Abstract 311.
- (23) Neubauer, H.; Cumano, A.; Muller, M.; Wu, H.; Huffstadt, U.; Pfeffer, K. Jak2 Deficiency Defines an Essential Developmental Checkpoint in Definitive Hematopoiesis. *Cell* **1998**, *93*, 397–409.
- (24) Garber, K. Pfizer's JAK Inhibitor Sails Through Phase 3 in Rheumatoid Arthritis. *Nat. Biotechnol.* **2011**, *29*, 467–468.

- (25) Jiang, J.; Ghoreschi, K.; Deflorian, F.; Chen, Z.; Perreira, M.; Pesu, M.; Smith, J.; Nguyen, D.-C.; Liu, E. H.; Leister, W.; Costanzi, S.; O'Shea, J. J.; Thomas, J. T. Examining the Chirality, Conformation and Selective Kinase Inhibition of 3-((3*R*,4*R*)-4-methyl-3-(methyl(7*H*-pyrrolo[2,3-*d*]pyrimidin-4-yl)amino)piperidin-1-yl)-3-oxopropanenitrile (CP-690,550). *J. Med. Chem.* **2008**, *51*, 8012–8018.
- (26) Flanagan, M. E.; Blumenkopf, T. A.; Brissette, W. H.; Brown, M. F.; Casavant, J. M.; Shang-Poa, C.; Doty, J. L.; Elliott, E. A.; Fisher, M. B.; Hines, M.; Kent, C.; Kudlacz, E. M.; Lillie, B. M.; Magnuson, K. S.; McCurdy, S. P.; Munchhof, M. J.; Perry, B. D.; Sawyer, P. S.; Strelevitz, T. J.; Subramanyam, C.; Sun, J.; Whipple, D. A.; Changelian, P. S. Discovery of CP-690,550: A Potent and Selective Janus Kinase (JAK) Inhibitor for the Treatment of Autoimmune Diseases and Organ Transplant Rejection. *J. Med. Chem.* **2010**, *53*, 8468–8484.
- (27) Williams, N. K.; Bamert, R. S.; Patel, O.; Wang, C.; Walden, P. M.; Fantino, E.; Rossjohn, J.; Lucet, I. S. Dissecting Specificity in the Janus Kinases: The Structures of JAK-Specific Inhibitors Complexed to the JAK1 and JAK2 Protein Tyrosine Kinase Domain. *J. Mol. Biol.* **2009**, *387*, 219–232.
- (28) Prior to the commencement of this work, a series of related, imidazolone-containing compounds had been described as JAK3 inhibitors: (a) Inoue, T.; Tanaka, A.; Nakai, K.; Sasaki, H.; Takahashi, F.; Shirakami, S.; Hatanaka, K.; Nakajima, Y.; Mukoyoshi, K.; Hamaguchi, H.; Kunikawa, S.; Higashi, Y. Heterocyclic Janus Kinase 3 Inhibitors. WO2007077949, 2007. More recently, during the course of this work, patent applications have appeared describing other tricyclic, azaindole-containing scaffolds as JAK inhibitors. These include azaindole annelated by pyrrole, (b) Shirakami, S.; Nakajima, Y.; Maeda, J.; Tominaga, H.; Yamagishi, H.; Hondo, T.; Inami, M.; Morio, H.; Inoue, T.; Mizutani, T.; Ishioka, H. Fused Pyrrolopyridine Derivative. WO2010119875, 2010; by pyrrole, pyrazole, and isoxazole, (c) Wishart, N.; Argiriadi, M.; Calderwood, D. J.; Ericsson, A. M.; Fiamengo, B. A.; Frank, K. E.; Friedman, M.; George, D. M.; Goedken, E. R.; Josephsohn, N. S.; Li, B. C.; Morytko, M. J.; Stewart, K. D.; Voss, J. W.; Wallace, G. A.; Wang, L.; Woller, K. R. Novel Tricyclic Compounds. WO2009152133, 2009; by isothiazole, triazole, and imidazole, as in 3, (d) Wishart, N.; Argiriadi, M.; Breinlinger, E. C.; Calderwood, D. J.; Ericsson, A. M.; Fiamengo, B. A.; Frank, K. E.; Friedman, M.; George, D. M.; Goedken, E. R.; Josephsohn, N. S.; Li, B. C.; Morytko, M. J.; Mullen, K. D.; Somal, G.; Stewart, K. D.; Voss, J. W.; Wallace, G. A.; Wang, L.; Woller, K. R. Novel Tricyclic Compounds. WO2011068899, 2011. Tricycles corresponding to 3 but having distinct substitution and probably employing an alternative hinge-binding mode have recently appeared as JAK2 inhibitors: (e) Purandare, A. V.; Grebinski, J. W.; Hart, A.; Inghrim, J.; Schroeder, G.; Wan, H. JAK2 Inhibitors and Their Use for the Treatment of Myeloproliferative Diseases and Cancer. WO2011028864, 2011.
- (29) Analogues of 1 substituted with pendent sulfonamides are described to have binding selectivity for JAK1 over JAK2 and JAK3: (a) Acker, B. A.; Hartmann, S. J.; Huang, H.-C.; Jacobsen, E. J.; Promo, M. A.; Wolfson, S. G.; Xie, J. Pyrrolo[2,3-*d*]pyrimidine Compounds. WO2011045702, 2011, and (b) Xie, J.; Promo, M. A.; Jacobsen, E. J.; Huang, H.-C.; Maddux, T. Pyrrolo[2,3-*D*]pyrimidine Compounds. WO2011075334, 2011. Also claimed as JAK1 selective inhibitors are derivatives of 2: (c) Huang, T.; Xue, C.-B.; Wang, A.; Kong, L.; Ye, H. F.; Yao, W.; Rodgers, J. D.; Shepard, S.; Wang, H.; Shao, L.; Li, H.-Y.; Li, Q. Piperidin-4-yl Azetidone Derivatives as JAK1 Inhibitors. WO2011112662, 2011; (d) Rodgers, J. D.; Li, Y.-L.; Shepard, S.; Wang, H. Heterocyclic Derivatives of Pyrazol-4-yl-pyrrolo[2,3-*d*]pyrimidines as Janus Kinase Inhibitors. WO2011028685, 2011; (e) Li, Y.-L.; Rodgers, J. D. 3-[4-(7*H*-Pyrrolo[2,3-*d*]pyrimidin-4-yl)-1*H*-pyrazol-1-yl]octane- or Heptane-nitrile As JAK Inhibitors. WO2010135621, 2010, along with a polyaryl macrocycle: (f) Combs, A. P.; Sparks, R. B.; Yue, E. W.; Feng, H.; Bower, M. J.; Zhu, W. Macroyclic Compounds and Their Use as Kinase Inhibitors. WO2009132202, 2009.
- (30) Van't Klooster, G.; Van Rompaey, L.; Menet, C.; Namour, F.; Vanhoutte, F.; van der Aar, E.; Clément-Lacroix, P.; Gallien, R.; Nelles, L.; Guérin, C.; Smets, B.; Brys, R.; Feyen, J.; Wigerinck, P. *Preclinical Pharmacology and Early Clinical Evaluation of GLPG0634, a Selective JAK1 Inhibitor for the Treatment of Rheumatoid Arthritis*. EULAR Annual European Congress of Rheumatology, London, May 25–28, 2011; BMJ Publishing Group Ltd.: London; Abstract 251.
- (31) Galapagos' GLPG0634 Shows Excellent Efficacy and Safety in Rheumatoid Arthritis Phase II Study. Galapagos NV: Mechelen, Belgium, Press Release November 22, 2011. Available at <http://www.glp.com/>.
- (32) Malerich, J. P.; Lam, J. S.; Hart, B.; Fine, R. M.; Klebansky, B.; Tanga, M. J.; D'Andrea, A. Diamino-1,2,4-triazole Derivatives Are Selective Inhibitors of TYK2 and JAK1 Over JAK2 and JAK3. *Bioorg. Med. Chem. Lett.* **2010**, *20*, 7454–7457.
- (33) Karaman, M. W.; Herrgard, S.; Treiber, D. K.; Gallant, P.; Atteridge, C. E.; Campbell, B. T.; Chan, K. W.; Cicero, P.; Davis, M. I.; Edeen, P. T.; Faraoni, R.; Floyd, M.; Hunt, J. P.; Lockhart, D. J.; Milanov, Z. V.; Morrison, M. J.; Pallares, G.; Patel, H. K.; Pritchard, S.; Wodicka, L. M.; Zarrinkar, P. P. A Quantitative Analysis of Kinase Inhibitor Selectivity. *Nat. Biotechnol.* **2008**, *26*, 127–132.
- (34) Van Abbema, A.; Kanada, H.; Chang, C.; Bir Kohli, P.; Smith, J.; Barrett, K.; Lewin-Koh, N.; Johnson, A. R.; Ghilardi, N.; Blair, W. Determination of the JAK-Dependence of Cytokine Pathways Using Small Molecule Inhibitors, unpublished results.
- (35) EC₅₀ values for compounds that do not achieve at least 50% inhibition at the highest concentration tested (10 μM) in the cell based assays are considered to be noncalculable and are reported as >10 μM. Owing to normal run-to-run variability, some weakly potent compounds achieve >50% inhibition in some, but not all, of the replicate runs. In these cases, we report EC₅₀ > X, where X is the arithmetic mean of all the individual EC₅₀ values, both calculable and noncalculable. For example, compound 13 displayed replicate EC₅₀ values of 6.3 μM, >10 μM, and >10 μM in the pSTAT5-EPO assay; thus, the average JAK2 cell EC₅₀ was reported as >8.8 μM, giving a JAK2/JAK1 cell selectivity of >6.3-fold.
- (36) Chrencik, J. E.; Patny, A.; Leung, I. K.; Korniski, B.; Emmons, T. L.; Hall, T.; Weinberg, R. A.; Gormley, J. A.; Williams, J. M.; Day, J. E.; Hirsch, J. L.; Kiefer, J. R.; Leone, J. W.; Fischer, H. D.; Sommers, C. D.; Huang, H.-C.; Jacobsen, E. J.; Tenbrink, R. E.; Tomasselli, A. G.; Benson, T. E. Structural and Thermodynamic Characterization of the TYK2 and JAK3 Kinase Domains in Complex with CP690550 and CMP-6. *J. Mol. Biol.* **2010**, *400*, 413–433.
- (37) As crystallization of JAK1 proved difficult during the early stages of this program, the cocrystallization of several compounds reported below was solved using a JAK2 triple mutant surrogate, in which three residues adjacent to the ligand binding site were mutated to the respective JAK1 residues (i.e., Q853R, Y931F, and D939E using JAK2 numbering) in order to explore potential binding interactions between these residues and the ligand. Later compounds in the series were successfully cocrystallized with wild type JAK1.
- (38) *The Pymol Molecular Graphics System*, version 1.3; Schrödinger, LLC: New York (<http://www.pymol.org>).
- (39) Wang, X.; Zhi, B.; Baum, J.; Chen, Y.; Crockett, R.; Huang, L.; Eisenberg, S.; Ng, J.; Larsen, R.; Martinelli, M.; Reider, P. A Practical Synthesis of 2-((1*H*-Pyrrolo[2,3-*b*]pyridine-4-yl)methylamino)-5-fluoronicotinic Acid. *J. Org. Chem.* **2006**, *71*, 4021–4023.
- (40) Vanotti, E.; Angelucci, F.; Bargiotti, A.; Brasca, M. G.; Menichincheri, M. Pyrrolopyridines as Kinase Inhibitors. WO2007054508, 2007.
- (41) Brown Ripin, D. H.; Abele, S.; Cai, W.; Blumenkopf, T.; Casavant, J. M.; Doty, J. L.; Flanagan, M.; Koecher, C.; Laue, K. W.; McCarthy, K.; Meltz, C.; Munchhof, M. J.; Pouwer, K.; Sha, B.; Sun, J.; Teixeira, J.; Vries, T.; Whipple, D. A.; Wilcox, G. Development of a Scalable Route for the Production of *cis*-*N*-Benzyl-3-methylamino-4-methylpiperidine. *Org. Process Res. Dev.* **2003**, *7*, 115–120.
- (42) Ramadas, K.; Srinivasan, N. Iron-Ammonium Chloride: A Convenient and Inexpensive Reductant. *Synth. Commun.* **1992**, *22*, 3189–3195.
- (43) Li, F.; Brogan, J. B.; Gage, J. L.; Zhang, D.; Miller, M. J. Chemoenzymatic Synthesis and Synthetic Application of Enantiopure

Aminocyclopentenols: Total Synthesis of Carbocyclic (+)-Uracil Polyoxin C and Its α -Epimer. *J. Org. Chem.* **2004**, *69*, 4538–4540.

(44) Ranganathan, S.; George, K. S. 2-Aza-3-oxabicyclo[2.2.1]-heptane Hydrochloride: An Exceptionally Versatile Synthon For Carbocyclic Sugars and Nucleosides. *Tetrahedron* **1997**, *53*, 3347–3362.

(45) Gregson, M.; Ayres, B. E.; Ewan, G. B.; Ellis, F.; Knight, J. 2,6-Diaminopurine Derivatives. WO199417090, 1994.

(46) Erickson, S. D.; Qian, Y.; Tilley, J. W. Diaminocyclohexane and Diaminocyclopentane Derivatives. WO2008065021, 2008.

(47) (a) Morrison, J. F. Kinetics of the Reversible Inhibition of Enzyme-Catalyzed Reactions by Tight-binding Inhibitors. *Biochim. Biophys. Acta* **1969**, *185*, 269–296. (b) William, J. W.; Morrison, J. F. The Kinetics of Reversible Tight-binding Inhibition. *Methods Enzymol.* **1979**, *63*, 437–467.

■ NOTE ADDED AFTER ASAP PUBLICATION

After this paper was published on the Web June 11, 2012, a change was made to ref 31. The corrected version was reposted June 15, 2012.